Supplementary materials and methods (Moen et al., *Proceedings of the Royal Society B*)

LOCALITIES AND FROG COLLECTION

Three localities were chosen to maximize representation of the phylogenetic history of microhabitat changes in frogs. These locations were Yunnan Province, China (where aquatic and semi-aquatic frogs are most diverse and have a deep history; [S1–S3]), the Amazon rainforest near Leticia, Colombia (where arboreal and terrestrial frogs are the most diverse and have a deep history; [S1–S3]), and the wet tropics of northern Australia near Darwin (dominated by two major clades, Myobatrachidae and Hylidae, the latter of which has radiated in situ to use diverse microhabitats; [S4]). These locations were all tropical, mesic sites. In principle we could have also included communities that represented the Nearctic and Palearctic frog faunas. However, including localities from these regions would likely capture little additional information, as many studies have shown that the Nearctic and Palearctic faunas are dominated by the same clades of microhabitat specialists included already. For example, North American and European frog faunas have members of the same clade of arboreal frogs (hylids) present in Australia, Asia, and South America [S5], the same terrestrial bufonids as in China and South America [S6], and the same semi-aquatic ranine ranid frogs as in the Asian tropics [S7]. Similarly, North American frog faunas contain the same clade of terrestrial microhylids present in South America and Asia [S8]. However, we acknowledge that each region does contain some unique clades and microhabitat types (e.g. burrowing pelobatids and scaphiopodids in Europe and North America, respectively) and that other regions of the world have important ecological radiations and clades and should be included in future studies (e.g. Africa, Madagascar).

Work in all three localities was done during each locality's wet season (June-July in China, December-March in Colombia, and November-January in Australia). Frogs in China

were collected in the general vicinity of Baoshan, Yunnan (25º 6.724' N, 99º 9.688' E), and performance trials were conducted at the Kunming Institute of Zoology, Chinese Academy of Sciences, in Kunming, Yunnan. Frogs in Colombia were primarily collected near Km. 11, Via Tarapacá (which runs north out of Leticia, Dept. of Amazonas; 4º 7.160' S, 69º 57.020' W). Performance trials were carried out within the Laboratorio de Productos Naturales at the Universidad Nacional de Colombia Sede Amazonia. Work in Australia was conducted at the University of Sydney's Tropical Ecology Research Facility (TERF) near Fogg Dam, Northern Territory, Australia (12º 34.735' S, 131º 18.862' E), and frogs were collected near the station. All work was conducted under Stony Brook University IACUC# 2011-1876 - NF.

At each site frogs were encountered primarily during dusk and into the evening via searches on foot (along forest paths, up streams, in ponds) or along the road. Frogs were collected by hand and placed in either cloth or plastic bags and transported directly to the laboratory after each evening's search. Upon arrival, frogs were individually housed within small plastic containers. Each container had abundant air holes and wet paper towels or grass to maintain moisture and provide shelter. In China and Colombia, containers were housed within the laboratory, whereas in Australia containers were placed in an outdoor shed.

Performance data were collected from each individual over the course of about one week, and afterward all individuals were sacrificed and preserved (see below). The sex of all individuals was internally verified through inspection of gonads, and morphological data were obtained from each individual (see separate sections below for more detail on performance and morphological methods).

Frog species were chosen so as to maximize sampling of microhabitat use, though search success limited which species were actually studied. As a consequence, not all microhabitat use

specialists were sampled from China and Colombia (though all types occur at each site; see [S9,S10]). The species used in this study and microhabitat use of each (see below) are listed in table S1.

As extra weight related to egg mass in females may affect jumping performance [S11], we primarily collected adult male frogs. However, due to low abundance in the field for some taxa or the inability to externally sex individuals, in some cases adult females were used. To see if sex influenced our results, we conducted a preliminary statistical analysis on jumping performance. We conducted a multivariate analysis of variance on our full data matrix (i.e. with all individuals instead of species means) that estimated the effects of species, sex, and a species-sex interaction term, with jumping peak velocity, peak acceleration, and peak power as the response variables. This model showed no effect of sex on jumping performance (sex main effect: $F_{3,149} = 2.0$, $P = 0.112$; sex-species interaction: $F_{81,453} = 0.9$, $P = 0.651$). As a consequence, we pooled data across sexes for all analyses.

Sample sizes for each species are given in tables S2 and S3, with a mean sample size of 4.98 and a range of 1–8. We note that we collected data for approximately 50% more individuals than presented here. As we were interested in capturing maximum performance (see below), we did not analyze data from individuals who performed submaximally, as was often apparent simply from their posture before or during jumping and swimming.

PERFORMANCE

Overview

For each individual we collected data on performance in jumping, swimming, and clinging. These behaviors were chosen because they are likely to be divergent across species using

different microhabitats. Jumping is arguably important for almost all species of frogs [S12–S15], but variation among species might be seen if trade-offs exist between jumping and other performance variables (e.g. swimming; [S16]). We expect swimming to be particularly important for semi-aquatic species and clinging should be important in arboreal or rock-climbing species [S17,S18]. Importantly, data on these three performance behaviors were measurable for all species despite differences in microhabitat use, whereas data on other potentially relevant behaviors such as burrowing were not collected because we simply could not elicit this behavior from most species.

In the case of jumping and swimming, we collected data on velocity, acceleration, and power (see details below). While endurance may be important in some species [S19,S20], we did not measure this as most species use rapid, maximal efforts during predator escape and prey capture ([S21]; but see [S19]) and hence tire quickly [S22,S23].

Jumping

Each individual frog underwent 3–5 jumping sessions, starting the day after collection. In each session, individuals were tested until performance was visibly reduced (i.e. leading to exhaustion), usually 4–5 individual jumps. Jumping sessions were conducted every other day (with swimming performance trials conducted on days in-between; see below). To control for potential activity differences due to time of day, all individuals were tested at least once each in the morning (0800–1200h), afternoon (1200–1800h), and evening (1800–0200h), the latter corresponding to peak activity time for most species. The order of testing individuals was randomized within a given jumping session. Over all sessions and trials, only the single jump that represented maximum performance of each individual over all jumping sessions was used as

data for further analysis (see below). These maximal efforts were not concentrated during any particular time of day; across all localities, 61 individuals performed maximally in the morning, 83 during the afternoon, and 74 in the evening. Furthermore, we conducted a multivariate analysis of variance with species, time, and a species-time interaction term as predictor variables, and peak jumping velocity, peak acceleration, and peak power as response variables. This analysis showed that our quantitative measures of performance were not influenced by the time of day at which that maximal effort was recorded (time main effect: $F_{3,138} = 0.4$, $P = 0.770$; time-species interaction: $F_{114,420} = 0.9$, $P = 0.712$). In other words, neither in general nor within a given species was peak performance related to time of day.

The complete takeoff phase of each jump was recorded on a TroubleShooter TS250MS (Fastec Imaging Corporation, 2004) high-speed video camera at 250 frames per second. This framing rate is generally appropriate for filming the jumps of small vertebrates [S11]. Complete jumps were not captured on film, and we were therefore not able to measure total distance, height of jump, or related variables. Filming complete jumps would have required zooming out an order of magnitude, which would have contributed to digitization error and thus an increase in the error of estimating velocity and acceleration profiles [S24]. However, all aspects of a jump are effectively captured during the takeoff phase – the takeoff angle, velocity, and leg length are the only variables that affect the height, time in the air, and total distance of a jump [S25], so we expect a very high correlation between these latter variables and those we measured. Jumping trials were conducted within an arena constructed of two Plexiglas panels (85 cm long by 60 cm wide, 14 cm apart). This formed a lane through which frogs jumped parallel to the camera so as to avoid underestimating velocity and acceleration due to lateral movement. The substrate of the arena was cardboard, though fine-grained sandpaper (1000-grit) was overlaid for toads of the

genera *Rhinella* and *Duttaphrynus* because their relatively dry skin did not gain traction on cardboard. We elicited maximum effort by placing frogs within the arena and either slapping a hand on the ground just behind the frog or lightly tapping the frog's back. We also placed a dark box at the end of the track to give each frog an escape target.

In China and Colombia, frogs were taken directly from their cages for performance trials, as they were also housed within the laboratory. In Australia, frogs were placed within the laboratory 1h before the start of performance trials to acclimate to ambient temperature. At the time of the start of each jumping session for each frog, ambient temperature near the frog's cage in the laboratory was noted. This temperature was always within the temperature range in which frogs were collected in the field for this study (results not shown; laboratory temperature ranges [in ºC] were 24.2–27.1 in Australia, 21.8–25.2 in China, and 23.5–27.6 in Colombia). These temperatures are also within the range of peak performance for tropical frogs (see review in [S26], their figure 3), and in general whole-organism performance in frogs seems to be less temperature sensitive than is muscle physiology per se [S27,S28]. Most importantly, an analysis of a subset of the data (Australian frogs) showed almost no relationship between temperature and jumping peak velocity, peak acceleration, and peak power (effect of temperature across all species: $P \geq 0.395$ in all analyses; temperature within species: $P \geq 0.301$ for peak velocity and acceleration). The one exception to these insignificant results was a significant interaction between species and temperature (i.e. within-species effect of temperature; $P = 0.050$) on peak power, driven largely by a negative relationship between temperature and peak power in *Litoria nasuta*. However, this association was in the direction opposite of that expected and also the only significant factor of 36 estimated parameters across these three models, suggesting that it may be due to chance alone. Finally, there was no tendency for the best performance for a given

individual (i.e. the data that were eventually used for statistical analyses) to occur at a particular temperature (results not shown).

Swimming

The general methodology for collecting data on swimming followed that for jumping (e.g. frequency of trials, time of day, and temperature). Burst swimming performance was elicited by releasing frogs at one end of a long aquarium (120 cm long by 30 cm wide by 50 cm tall) filled with water to a depth of 30 cm. Swimming performance was captured from above using the same camera as for jumping performance but at 125 frames per second, due to the slower speeds and accelerations associated with swimming. As some species had a tendency to dive instead of swim horizontally on the surface, the angle of all dives was noted so as to convert the distance traveled in the plane of the camera to actual distance traveled (i.e. $D_{actual} = D_{camera} / \cos(\theta)$).

Clinging

We designed a clinging apparatus by gluing a metal hinge to the bottom of a Teflon®-coated non-stick frying pan (28.5 cm diameter, 6 cm deep). This surface was used because high molecular weight plastics (including Teflon®) have a similar coefficient of friction to the waxy leaves typical of rainforest trees ([S18]; see also [S29,S30]). Frogs were placed on the pan when it was level, and the pan was gradually inverted from 0º up to 180º. The angle of the pan was noted at the moment in which each individual lost traction (via either sliding or falling, depending on the angle). Each frog was tested 3 times to ensure accurate estimation of maximum adhesive performance [S18]. Data used for subsequent analyses were only the maximum angle attained by each individual across all trials. As in jumping, we do not expect

temperature to have strongly affected our maximum clinging angle estimates. Wet adhesion, as is used by frogs to cling to surfaces [S17], is governed by two primary forces [S31]. First, Stefan adhesion is related to viscosity of the fluid, which is directly related to temperature, but it likely plays a very small role frog adhesion [S17]. On the other hand, capillarity is temperature independent, and this second force plays the largest role in frog adhesion [S17,S18].

Data extraction from videos and performance variables

The tip of the snout was digitized in each video frame for the takeoff phase in jumping and burst-effort in swimming (i.e. complete swimming stroke). This was generally 2 frames before each effort and several frames (usually 4–5) after, thus allowing for adequate characterization of all aspects of performance (e.g. maximum horizontal velocity and acceleration are not alterable after takeoff; [S25]). Digitization was done in ImageJ (Ver. 1.42; [S32]) using the "Figure Calibration" plug-in (F. V. Hessman, http://www.astro.physik.uni-goettingen.de/~hessman/ImageJ/Figure_Calibration/). Changes in vertical and horizontal position of digitized coordinates between frames were then converted into straight-line distance traveled between each frame. Distance-time plots were then uploaded into QuickSAND [S24] to smooth the plots and subsequently calculate velocity and acceleration profiles via numerical derivatives, using quintic spline algorithms from Woltring [S33]. These algorithms smooth through distance-time data by optimizing smoothness not only in the original distance-time plots but also in the derivatives, based on the expectation that animal performance curves (such as those of velocity and acceleration) should be relatively smooth. Ideally one would use an objective criterion to smooth through the data. However, the only fully automatic smoothing algorithm in QuickSAND (generalized cross-validation; GCV) frequently seemed unstable and

produced biologically unrealistic curves (e.g. positive acceleration after jumping takeoff or during gliding in swimming). Therefore, we manually adjusted the smoothing parameter until we achieved the least amount of smoothing possible while also reaching velocity and acceleration profiles that were realistic (see [S34,S35] for examples of these characteristics).

We examined the following jump variables, following Toro et al. [S36] and Kuo et al. [S11]: (i) takeoff angle (measured directly in ImageJ), (ii) peak takeoff velocity, (iii) peak acceleration during takeoff, and (iv) peak mass-specific power during takeoff (maximum value of the product of the instantaneous velocity and acceleration profiles; [S36]). In swimming, we calculated (i) peak velocity, (ii) peak acceleration, and (iii) peak mass-specific power. Finally, as mentioned above, our sole performance variable for clinging was maximum clinging angle.

For each of these variables, we obtained a maximum value for each individual and then averaged maximum values among individuals of a species to obtain a mean value for each performance variable for each species (table S2). Although variables characterizing maximum performance were generally consistent within individuals (e.g. peak velocity and peak acceleration for a given individual were achieved in the same video), this was not always the case. However, because of the inter-dependence of many of these performance variables (i.e. a combination of the "best" values may not be biologically possible for an individual in a single effort), we chose to use the single video characterized by the peak velocity of a given individual as its maximum performance instead of taking the maximum values across all videos. Nonetheless, species means were nearly identical regardless of how we characterized an individual's maximum performance (e.g. jumping peak velocity: $r = 0.9991$; jumping peak acceleration: $r = 0.9949$; jumping peak power: $r = 0.9997$).

208 ***MORPHOLOGY***

209 After all performance trials had been completed at a given site, all frogs were euthanized and
210 preserved in either formalin (Australia, China) or 70% ethanol (Colombia), depending on
211 availability. After fixation, all specimens were later placed in 70% ethanol for long-term storage.
212 With the exception of toepads and webbing (see next paragraph), all morphological data were
213 taken from preserved specimens.

214 Photos were taken of the hands and feet of each individual immediately after
215 euthanization to measure the area of inter-digit webbing, area of toe tips (e.g. enlarged toepads in
216 arboreal frogs or the circular distal end of the toe in species without obvious toepads), and area
217 of the inner metatarsal tubercle (which is often enlarged and used as a spade for digging in
218 burrowing species; [S37]). For each photo either the left hand or left foot was placed against a
219 flat glass plate and photos were taken by either a Canon Powershot A590 IS (China, Colombia)
220 or a Canon Rebel T1i digital SLR camera fitted with a 100mm macro lens (Australia). Areas of
221 inter-digit webbing, tips of digits, and metatarsal tubercle were measured in ImageJ through
222 digitizing the circumference of each structure, and sums of individual webbing or digit tips were
223 taken across the entire foot or hand as an estimate of area for data analysis. Inter-digit webbing
224 of the hands was absent in most species, so we eliminated this variable from further analysis. In
225 most individuals photos of hands and feet were taken immediately after sacrificing them (i.e.
226 before preservation). In a subset of the individuals, doing this procedure immediately after death
227 was not logistically possible (due to mechanical failure of camera equipment), so this procedure
228 was done after preservation. To test for any systematic differences between area estimates from
229 preserved and freshly euthanized specimens, we took photographs of both states for a subset of
230 frogs from Colombia. A paired t-test showed consistent differences between preserved and

freshly euthanized frogs in the estimated sizes of toe and finger tips for these frogs, though not for webbing (n = 4 species and 32 individuals; toe tips: t = -4.97, $P < 0.001$; finger tips: t = -5.29, $P < 0.001$; foot webbing: t = -1.40, P = 0.172; hand webbing: t = 1.65, P = 0.109). This difference was likely due to the tendency for toe and finger tips to pull back slightly and become concave when they are naturally adhering to the glass plate, particularly in taxa with enlarged discs (i.e. this is how they function to stick to smooth surfaces in live frogs; [S17]), resulting in lower estimates of toe tip size in freshly killed specimens. Nonetheless, because this relationship was consistent within and across species, we corrected for differences between freshly euthanized and preserved specimens by estimating the fresh size of toe and finger tips for preserved specimens using the following equations: (i) foot toe tips: $A_f = 0.6873A_p$, $R^2_{adj} = 0.993$; and (ii) finger tips: $A_f = 0.8224A_p$, $R^2_{adj} = 0.990$ (where A_p = size of area on preserved specimens, A_f = area on fresh specimens, and equations estimated across all 32 individuals regardless of species).

Next, we measured 10 external variables of functional significance [S16,S25]. These were: (i) snout-to-urostyle length (SUL; tip of snout to posterior end of urostyle); (ii) femur length (tip of urostyle to knee); (iii) tibiofibula length (tip of knee to tip of heel / proximal end of the tarsus); (iv) tarsus length (tip of heel to proximal edge of inner metatarsal tubercle); (v) foot length (proximal edge of inner metatarsal tubercle to distal end of outstretched fourth toe); (vi) head length (posterior corner of jaw to tip of snout); (vii) head width (distance between posterior corners of jaw); (viii) humerus length (tip of elbow to insertion point at the body wall); (ix) radioulnar length (distal edge of outer palmar tubercle to elbow); and (x) hand length (distal edge of outer palmar tubercle to tip of third finger). These variables were chosen so as to reflect variation in overall body size (variable i), relative hindlimb length (vars. ii–v) and forelimb

length (vars. viii–x), and head shape (vars. vi–vii). So as to reduce redundancy in our data and because preliminary analyses showed little variation among species in individual elements of the hindlimbs and forelimbs, we summed those sets of variables (vars. ii–v and viii–x, respectively) to produce a single measurement for each limb. All external linear measurements were made on preserved specimens.

Finally, the muscle mass of the left hindlimb was quantified in each individual after preservation because of the large role that hindlimb muscle mass plays in performance in frogs [S28]. The two major muscle groups of the legs (those associated with the femur and the tibiofibula) were dissected out of the left leg via cutting at the origin and insertion points of these muscles. These muscle groups were chosen because they contain the major extensors used in jumping and swimming (primarily the plantaris longus on the lower leg and various muscles on the upper leg [S16,S25,S35]). Muscles were then gently patted dry and weighed on a mass scale accurate to 0.01g (China) or 0.001g (Colombia, Australia). Species means were calculated for each variable and were used for all subsequent statistical analysis (table S3).

Some studies have shown changes in measurements done before and after preservation in frogs, thus questioning the utility of preserved specimens [S38,S39]. However, we are interested in relative differences among species and any possible effects of preservation should not introduce systematic error that would affect interspecific comparisons. This is supported by Deichmann et al. [S39], who showed that the absolute reduction in snout-to-urostyle length (SUL) across 14 species was proportional to SUL itself (i.e. relative differences among species were maintained after preservation).

MICROHABITAT USE

We gathered data on microhabitat use from the literature. We placed each species into one of four broad categories: (i) arboreal (typically found above ground level on vegetation), (ii) aquatic/semi-aquatic (generally found in or adjacent to water bodies, such as ponds or streams), (iii) terrestrial (generally found far from water and on the ground), and (iv) burrowing (digs its own burrows with rear feet; note that some frogs burrow head-first [S37,S40,S41], but none were included in this study). We categorized species primarily based on adult activity outside of the breeding season. Behavior associated with breeding was not considered here because most species in this study associate with water for breeding but would not all be considered aquatic or semi-aquatic. We note that many burrowing frogs may not be active in their burrows (and might therefore be considered terrestrial instead), but we nevertheless use this category to include this potentially important behavior, as it involves distinct selection pressures (and hence adaptations) not found in other frogs [S37].

In most cases, literature sources also categorized these species using the same category names listed above. For those species whose designations were unclear, we placed them within a category based on behavioral descriptions in the literature. Additionally, we verified these designations during fieldwork. The one exception to this was for burrowing species, which were usually encountered above ground, as encountering such species in burrows or in the act of burrowing is exceptionally rare. Data on microhabitat use are listed in table S1.

PHYLOGENY

We used three approaches to obtain a phylogeny and branch lengths for comparative analyses. First, we used the maximum likelihood phylogeny and branch lengths from Pyron and Wiens [S42], which is the most comprehensive analysis of anuran phylogeny to date, after deleting

unsampled species. Second, we estimated a time-calibrated phylogeny using the Bayesian uncorrelated lognormal approach (in BEAST; [S43,S44]) and using the molecular data assembled by Pyron and Wiens [S42]. However, for this analysis, we constrained the topology to that of Pyron and Wiens [S42] to reduce potential errors in the topology associated with limited taxon sampling. Third, we used the same data and method (BEAST) to simultaneously estimate the phylogeny and divergence times. This latter approach allowed us to incorporate uncertainty in both the phylogeny and branch lengths.

The data set of Pyron and Wiens [S42] consisted of 12 genes (3 mitochondrial and 9 nuclear), including 16S (up to 1,855 bp per species), 12S (1,230 bp), RAG-1 (2,697 bp), cyt-*b* (1,140 bp), TYR (600 bp), RHOD (315 bp), SIA (397 bp), POMC (651 bp), CXCR4 (753 bp), H3A (328 bp), NCX1 (1,335 bp), and SLC8A3 (1,132 bp). These data were compiled from many previous studies of amphibian phylogeny that utilized this partially overlapping set of genes. Not all genes have data for all species, but this appears to have little impact on the phylogenetic analyses [S42,S45].

Some of the species used in the performance analyses were not included in the molecular data set of Pyron and Wiens [S42]. However, most species were easily accommodated by utilizing species included in the data matrix that appear to be closely related to the species sampled for performance, ecological, and morphological data. Specifically, we made the following replacements. (i) *Amolops mantzorum* (molecular) for *A. tuberodepressus* (performance), given that some authors consider *A. tuberodepressus* to be a synonym of *A. mantzorum* [S46]. (ii) *Calluela guttulata* (molecular) for *Calluela yunnanensis* (performance), the only *Calluela* included in the tree of Pyron and Wiens [S42]. (iii) *Chiasmocleis shudikarensis* (molecular) for *C. bassleri* (performance), an arbitrary selection between the two

Chiasmocleis in the tree of Pyron and Wiens [S42]. (iv) *Hypsiboas sibleszi* (molecular) for *H. hobbsi* (performance), given that both are members of the *Hypsiboas punctatus* group [S47]. (v) *Hypsiboas cinerascens* (molecular) for *H. punctatus* (performance), given that both are in the *H. punctatus* group [S47] and are very similar morphologically. (vi) *Rhinella dapsilis* (molecular) for *Rhinella proboscidea* (performance), given that both belong to the complex of species referred to as *Rhinella margaritifera* [S47]. (vii) *Uperoleia laevigata* (molecular) for *U. lithomoda* (performance), given that *U. laevigata* is one of only two *Uperoleia* species in the molecular data set. Finally, although *Limnodynastes convexiusculus* is in the tree, we used *L. salmini* to represent this taxon given its better sampling of genes. Given the broad phylogenetic and temporal scale of this study, these congeneric replacements should have little impact on the estimated topology and branch lengths.

Analyses with BEAST (v1.5.4) utilized the following settings. Following Pyron and Wiens [S42], we used a separate partition for each gene (with unlinked substitution models but with the clock model and tree model linked across genes). We used the GTR+I+Γ model for each gene (general time reversible with parameters for invariant sites and a gamma distribution of rates among variable sites), with estimated base frequencies and 4 rate categories for variable sites. Protein-coding genes were each partitioned based on codon positions, and ribosomal genes (12S and 16S) were each partitioned based on stems and loops. Substitution and rate heterogeneity parameters were unlinked across these partitions. Dating analyses used an uncorrelated lognormal relaxed clock with an estimated rate. For the unconstrained analysis, a Yule speciation model was used. Given that our sampling of species spanned relatively few of the most relevant fossil taxa for dating, we used previously estimated dates for two important clades as priors (Hyloidea, Ranoidea). We used the estimated ages from the penalized likelihood

346 analysis of Wiens [S48], which utilized an extensive set of fossil calibration points and a slow-
347 evolving nuclear gene. Similar dates were estimated for these two clades using alternate
348 methods and several nuclear and mitochondrial genes [S1]. Specifically, we used a normal prior
349 on the ages of these clades, with a mean of 73.5 Myr for Hyloidea and 111.9 for Ranoidea. We
350 used an arbitrary standard deviation of 5 Myr, yielding a 95% prior interval of 65.3–81.7 Myr for
351 Hyloidea and 103.7–120.1 Myr for Ranoidea.

352 For the constrained analyses, we set the monophyly of all clades to match Pyron and
353 Wiens [S42], an analysis based on the same genes but including >2,800 taxa. For the
354 unconstrained analysis, no clades were set to be monophyletic. Each analysis was run for 50
355 million generations, sampling every 1000 generations. A burn-in of 5 million generations (first
356 10%) was used. For the unconstrained analysis, we ran two replicate analyses and combined the
357 results, and we ran three replicate analyses for the constrained analysis.

358 Results were checked using Tracer v1.5.4 [S44]. For all analyses, the effective sample
359 size (ESS) for estimated dates was >200 in all replicates (although other parameters had ESS <
360 200). In addition, mean estimates for major clades (e.g. the root, Bufonidae, Dendrobatidae,
361 Hylidae, Microhylidae, Ranidae) for replicate analyses were very similar (e.g. within 1 Myr of
362 each other). This concordance strongly suggested that the estimated dates were stable. For the
363 constrained analyses, the final set of dates was taken from the third replicate (which had the
364 highest mean likelihood). A set of trees with branch lengths was subsampled every 100,000
365 generations from this analysis for comparative analyses, leaving a set of 450 post-burn-in trees.
366 These trees had identical topologies but somewhat different branch lengths. A consensus tree of
367 these post-burn-in trees is presented in figures 1 and S3, and this tree was used for further
368 comparative analyses.

For the unconstrained analyses, the two replicate analyses also gave very similar estimates of topology and clade support (posterior probabilities). We combined the results of the two replicate analyses using LogCombiner v1.5.4 [S44]. We again subsampled the trees every 100,000 generations, leaving 900 post-burn-in trees for comparative analyses. The majority-rule consensus of the post-burn-in trees showed notable differences with the likelihood tree of Pyron and Wiens [S42] and other studies, including non-monophyly of Hylidae and of the clade of Bufonidae+Dendrobatidae. However, these unusual relationships are only weakly supported. Although these trees may not represent the best possible estimate of topology for these species, the variation in topology allowed us to estimate the robustness of our results to a reasonable alternative topology, as we used the consensus tree for preliminary comparative analyses (see below).

DATA ANALYSIS

Principal components analysis

We first conducted principal components analysis (PCA) on both the performance and morphological data across all species in the study. We did this for two reasons. First, we wanted to account for redundancy in our data, as we expected most traits to scale with size, as is common for both morphology (e.g. [S49,S50]) and performance [S13,S51,S52]. Second, we used PCA to isolate this variation in body size from size-independent variation, as we were primarily interested in non-size-related variation among species within locations and across different microhabitats, given that large size variation occurred within all microhabitat categories (see *Relationship of microhabitat use to morphology and performance* below). Morphological data were first ln-transformed to achieve homogeneity of variances and ensure linear

392 relationships among variables. PCAs were conducted on the correlation matrices of traits
393 (instead of covariances; see [S53]), given that (i) morphological data consisted of linear, area,
394 and mass measurements, and (ii) performance data represented various scales of measurement
395 (e.g. velocity, acceleration, power, and angle).

396 We carried out both a standard PCA and a phylogenetic PCA, the latter following Revell
397 [S54]. Both procedures were carried out in R ver. 2.15 [S55], and phylogenetic PCA was
398 conducted with the package *phytools* [S56]. Given that both procedures gave similar results (e.g.
399 vector correlation of 0.9996 between the eigenvectors of morphological PC1 from standard PCA
400 and phylogenetic PCA using the BEAST constrained tree; vector correlations of morphological
401 PC1 among all three trees and standard PCA ranged from 0.9993–0.9999), we used PC scores
402 from the phylogenetic PCA for all subsequent analyses. All PC axes were retained for further
403 analyses instead of using a procedure to determine "significant" axes (such as in [S57]). We
404 chose to retain all axes because (i) variation explained by each axis did not decrease drastically
405 as PC dimensions increased (table S4); (ii) there was no inherent computational advantage to
406 dropping axes; and (iii) given that sample sizes for some microhabitat categories were low
407 relative to others (e.g. 4 semi-aquatic and 5 burrowing species versus 17 terrestrial and 18
408 arboreal species), ecologically important variation could lie in higher dimensions simply because
409 fewer species contributed to that variation (and thus its low contribution to total variation would
410 push it to higher PC dimensions). In sum, we retained all PC axes so as to fully characterize
411 variation among species and microhabitat categories. However, we note that we obtained
412 qualitatively similar results in all subsequent analyses when using only principal components 1–4
413 (in both morphology and performance), retained based on the Parallel Analysis approach of
414 Franklin et al. [S57].

Herein we interpret our results for principal components axes obtained with phylogenetic PCA using our second phylogeny (time-calibrated, topology constrained; see above and figure 1), which formed the basis of our subsequent statistical tests. As expected, PC1, which primarily represents an overall scaling axis, accounted for a large part of the variation in our data (82.8% in morphology and 56.4% in performance; table S4). The high similarity in magnitude and direction of individual elements of the eigenvectors for PC1 were consistent with this being a representation of overall size variation in morphology (mean ± SE: 0.32 ± 0.01). Likewise, PC1 for performance showed similar weights across most variables (0.37 ± 0.02, with the exception of clinging angle, which was small and negative [-0.06]) and represented overall high performance in jumping and swimming.

For morphology, PC2 represented variation in the size of toe and fingertips as well as foot webbing (table S4). PC3 largely represented variation in foot webbing, partly as a contrast with toe and fingertips. Finally, PC4 primarily showed large negative weights for head and leg length, contrasted with a large positive weight for metatarsal tubercle size (table S4). Figure S1 shows how species cluster in morphological PC space in PC2–4, chosen for ease of visualization and because these three PC axes represent the largest non-size-based variation. For brevity, we refer readers to table S4 for the interpretation of higher PC axes.

For performance variables, PC2 essentially showed a contrast between jumping and swimming performance (i.e. peak jumping acceleration, peak jumping power, jumping angle, and clinging angle, versus peak swimming velocity, peak swimming acceleration, and peak swimming power; table S4). PC3 largely represented variation in clinging angle, while PC4 represented variation in jumping takeoff angle (table S4). Figure S2 shows how species cluster

437 in performance PC space. As in morphology, for brevity we refer readers to table S4 for the
438 relationship between original variables and the higher PC axes.
439
440 **Relationship between morphology and performance**
441 Most large-scale tests of adaptive convergence thus far have primarily focused on patterns of
442 morphological convergence (e.g. [S58–S60]). While these studies have been very useful, whole-
443 organism performance capacities (e.g. locomotion, feeding) are expected to be the target of
444 selection in comparisons of fit to the environment, with morphology only selected upon
445 indirectly [S61–S64]. Furthermore, the relationship between morphology and performance may
446 not often be one-to-one [S64–S66], and this decoupling may allow for morphological diversity
447 where little exists in performance, or vice versa [S67,S68]. As a consequence, we tested a series
448 of relationships between our morphological and performance variables to examine whether our
449 data fit well-established biomechanical relationships, given that many such relationships have
450 been estimated within species (e.g. [S16]) or within a specific type of microhabitat specialist or
451 clade (e.g. arboreal rhacophorid frogs; [S18]) but not for multiple performance traits across many
452 species that use different microhabitats.
453 All analyses were phylogenetic generalized least-squares analyses assuming Brownian
454 motion [S69], and all size-independent (i.e. "relative") variables were estimated using the
455 phylogenetic size-correction procedure of Revell [S54] in the package *phytools* in R [S56]. We
456 note that although we assumed Brownian motion, we also conducted all analyses using an
457 Ornstein-Uhlenbeck (OU) model of evolution [S70,S71], with the alpha parameter of the OU
458 model estimated separately for each character and averaged across characters to specify the
459 correlation structure for each regression. We found qualitatively identical results for all analyses

460 regardless of the evolutionary model employed, so for simplicity we only report the results from
461 tests conducted under Brownian motion.

462 We first examined the relationship between body size, the sum of toe- and finger-tip size,
463 and clinging angle in a linear model, with the first two variables as predictors of the third.
464 Biomechanical principles dictate that for a given body size, increased toe-tip size should result in
465 a higher clinging angle due to the increased force of adhesion [S17,S18]. Additionally, body size
466 itself should reduce clinging angle, because mass multiplied by acceleration due to gravity is the
467 force that causes separation of a frog from its substrate [S18]. We conducted this analysis on
468 two sets of taxa. The first set was all species in this study. The second set was composed of just
469 the arboreal taxa with expanded toe pads, as this group most clearly was using only the toe pads
470 for adhesion (i.e. as compared to other taxa with small toe tips, who often achieved adhesion via
471 pressing their venter against the substrate). As expected, we found that both overall body size
472 (SUL) and relative toe-tip size were both strongly related to maximum clinging angle, with angle
473 negatively related to SUL and positively related to toe-tip size (SUL: $F_{1,41} = 59.66$; $P < 0.001$;
474 relative toe-tip size: $F_{1,41} = 36.03$; $P < 0.001$). We found the same results when we looked only
475 within arboreal taxa (SUL: $F_{1,15} = 47.29$; $P < 0.001$; relative toe-tip size: $F_{1,15} = 11.98$; $P =$
476 0.004).

477 Next, we examined the relationship between relative muscle mass in the hindlimb versus
478 acceleration and power in both jumping and swimming. Muscle mass is very important for
479 producing force (and in turn, acceleration and power) during jumping across all animals [S28].
480 Hence, we would expect that higher muscle mass leads to greater power and acceleration. We
481 conducted these analyses across all species, given that there is no clear reason why this
482 relationship should be affected by microhabitat use. For this analysis, we conducted four

483 regressions, all with relative muscle mass and SUL as the predictor variables: (i) peak jumping
484 acceleration; (ii) peak jumping power; (iii) peak swimming acceleration; and (iv) peak
485 swimming power. Relative muscle mass was strongly positively related to jumping acceleration,
486 whereas body size was negatively related (relative muscle mass: $F_{1,41} = 19.62$, $P < 0.001$; SUL:
487 $F_{1,41} = 11.77$, $P = 0.001$). Jumping power was independent of body size but positively correlated
488 with muscle mass (SUL: $F_{1,41} = 0.42$, $P = 0.522$; relative muscle mass: $F_{1,41} = 15.07$, $P < 0.001$).
489 The same relationships were found in both swimming acceleration (SUL: $F_{1,41} = 5.47$, $P = 0.024$;
490 relative muscle mass: $F_{1,41} = 27.01$, $P < 0.001$) and power (SUL: $F_{1,41} = 0.39$, $P = 0.534$; relative
491 muscle mass: $F_{1,41} = 45.07$, $P < 0.001$).

492 We also examined the relationship between relative muscle mass, relative leg length, and
493 peak jumping velocity. As noted above, acceleration is increased via higher force output by the
494 legs, and force output is related to muscle mass [S25,S28,S35]. All things being equal, higher
495 acceleration should lead to higher takeoff velocity; thus, higher muscle mass should result in
496 higher takeoff velocity as well. Additionally, relatively longer legs increase the time of the
497 takeoff phase of jumping, and if we assume that acceleration is held constant, a longer takeoff
498 phase will result in a higher peak velocity during takeoff [S25,S34]. Thus, we predicted a
499 positive relationship between relative muscle mass and peak jumping velocity, and likewise a
500 positive relationship between relative leg length and peak jumping velocity. We therefore
501 estimated a single model in which peak jumping velocity was regressed on relative leg muscle
502 mass, relative leg length, and snout-to-urostyle length (SUL). SUL was put into the model to
503 control for variation simply due to overall size, given that the latter is often positively correlated
504 with takeoff velocity [S51,S52]. These analyses showed that body size, relative muscle mass,
505 and relative leg length all are positively correlated with peak jumping velocity, though muscle

506 mass was not quite statistically significant (SUL: $F_{1,40} = 10.86$; $P = 0.002$; relative muscle mass:
507 $F_{1,40} = 3.16$; $P = 0.083$; relative leg length: $F_{1,40} = 21.24$; $P < 0.001$). Interestingly, the
508 correlation between relative muscle mass and leg length was negative ($r = -0.530$; $P < 0.001$),
509 suggesting that across species, jumping velocity can be increased either by increased muscle
510 mass or increased leg length, but usually not via both.

511 We chose to emphasize an analysis of variables individually (as above), so as to test
512 morphology-performance relationships found in previous studies of functional morphology
513 within and across frog species. However, one can also assess the overall multivariate
514 relationship between morphology and performance. To do this, we examined the covariation
515 between morphology and performance across all species by conducting a two-block partial least
516 squares analysis (2B-PLS; [S72]). This is a multivariate approach that constructs linear
517 combinations of the original variables in a way that best describes the covariation among sets of
518 the original variables – in this case, morphological and performance variables. Although the
519 general aim of 2B-PLS is similar to the more familiar canonical correlation analysis (CCA; [53]),
520 we chose to use the former because CCA may not necessarily produce linear combinations of
521 variables that account for the most covariance among datasets [S72].

522 In a two-block partial least squares analysis, one takes either a correlation or covariance
523 matrix of the original variables, defines a submatrix of correlations or covariances only among
524 variables of different sets (i.e. $\mathbf{R}_{12}$ of [S72]), and uses a singular-value decomposition [S73] to
525 decompose this submatrix into the product $\mathbf{F}_1\mathbf{D}(\mathbf{F}_2)'$. The matrix $\mathbf{D}$ is a diagonal matrix of
526 singular values, while $\mathbf{F}_1$ contains the weights for the linear combinations of the original
527 variables of the first set (here, morphological data) and $\mathbf{F}_2$ likewise contains the weights for the
528 second set (here, performance data). These weights can be used to interpret the contribution of

529 the original variables to each of the latent (new) variables of the 2B-PLS, while the singular
530 values indicate the strength of covariance among the latent 2B-PLS variables in each dimension
531 [S72].

532 Consistent with the above morphology-performance analyses, we first size corrected
533 morphological variables to isolate size-related versus size-independent variation in morphology.
534 In this case, size was represented by log-transformed snout-to-urostyle length, while all other
535 variables were residuals from a phylogenetic regression of the original (ln-transformed) values
536 on ln-transformed snout-to-urostyle length [S54]. Performance variables were simply ln-
537 transformed. All 2B-PLS calculations were done directly in R using a singular-value
538 decomposition of the correlation matrix of our data, following Rohlf and Corti [S72], and
539 statistical significance of individual 2B-PLS axes (and hence the overall relationship between
540 morphology and performance) was tested using the permutation procedure outlined in Rohlf and
541 Corti [S72], coded directly in R by us for this paper. We conducted tests of statistical
542 significance on both phylogenetically transformed data and untransformed data, finding similar
543 results. However, we present below the results of the untransformed data because interpretation
544 of the axes was simpler and also because not accounting for phylogeny does not bias parameters
545 that describe linear relationships among variables (as here; [S74,S75])

546 The two-block partial least-square analysis showed three axes of covariation between
547 morphology and performance that were greater than expected from random covariation
548 (dimensions 1–3: all $P = 0.001$; dimensions 4–8: all $P > 0.102$). Scores for morphology and
549 performance also showed relatively high correlations in these dimensions (table S5). Specific
550 loadings of original variables on the 2B-PLS variables showed that these multivariate results
551 were largely consistent with the above analyses based on functional predictions. The first

552 dimension reflected a positive relationship between relative leg length and performance in
553 jumping and swimming (table S5). Dimension 2 primarily represented the relationship between
554 morphology and clinging ability, with overall body size negatively related and relative toe- and
555 finger-tip area positively related. Dimension 3 generally showed that large overall body size was
556 negatively related to peak jumping acceleration and takeoff angle, but positively related to both
557 jumping and swimming peak velocity.
558
559 **Relationship of microhabitat use with morphology and performance**
560 A statistically significant relationship between microhabitat use and both morphology and
561 performance is first necessary in order to ask how microhabitat diversification (or lack thereof)
562 influences the evolution of morphology and performance (see following sections). Thus, we
563 next conducted one-way MANOVAs on the relationship between microhabitat use and the PC
564 scores in morphology and performance. All MANOVA models were estimated in R using the
565 function 'Wilks.test' in the package *rrcov* [S76], and PC scores were phylogenetically
566 transformed following the procedure outlined in Blankers et al. [S77]. Preliminary univariate
567 ANOVAs showed that microhabitat specialists were not distinguishable in terms of size
568 (morphology PC1: $F_{3,40} = 0.052$, $P = 0.984$) or overall jumping and swimming performance
569 (performance PC1: $F_{3,40} = 1.402$, $P = 0.256$), so MANOVAs were only conducted on PCs
570 beyond PC1 so as to focus on "size-independent" variation. Likewise, we only considered these
571 higher axes (i.e. PC2–10 for morphology, PC2–8 for performance) in remaining analyses so as to
572 focus on those axes of variation that distinguish microhabitat specialists. Finally, we conducted
573 preliminary two-way analyses including location as an additional term in the model to control for

location-specific factors (whether biological or experimental). As the variance among locations was lower than the error variance (both *P*-values > 0.50), we did not consider it further.

For four species with insufficient microhabitat use data (*Microhyla fissipes*, *Rhacophorus rhodopus*, *Rhinella margaritifera*, and *Rhinella proboscidea*), we assigned microhabitat use based on the microhabitat use of closely related species that were previously synonymous with our taxa (table S1). It is possible that this procedure could influence our test of the fits between microhabitat use and morphology, and between microhabitat use and performance. To control for this possibility, we re-ran our models without these four taxa. We found nearly identical results, with microhabitat use explaining even more variation in morphology without these data-deficient taxa (Wilks' lambda = 0.110; $P < 0.001$). We also obtained the same results for performance (Wilks' lambda = 0.309; $P = 0.009$). Vector correlations between the parameter estimates (table S6) of all taxa versus those estimated without the four data-deficient taxa further showed that using these taxa did not influence our analyses (morphology: arboreal $r_{vec} = 0.999$, terrestrial $r_{vec} = 0.996$; performance: arboreal $r_{vec} = 0.986$, terrestrial $r_{vec} = 0.813$; all semi-aquatic and burrowing species were in both analyses).

Patterns of in situ evolution and ecologically conservative dispersal of microhabitat use across assemblages

The major goal of our study was to understand the processes generating similarity in ecology (microhabitat), morphology, and performance across assemblages. Following the conceptual framework of Moen et al. [S50], we considered two general processes as explaining the ecological traits of each species in each assemblage. First, if an ecological character state (e.g. microhabitat) evolved within a region (i.e. in a clade endemic to the region), its presence there in

that clade was considered as being due to in situ evolution (ISE). Alternatively, a character state can evolve in a clade outside of the region, but dispersal of a lineage from that clade into the region can add that character state to the region. Because this dispersal into the region occurs without concomitant character change, we call this origin into the region ecologically conservative dispersal (ECD), following the terminology of previous authors [S50,S78]. We first considered microhabitat states in each assemblage in terms of ISE and ECD and then tested hypotheses relating these processes to variation in morphology and performance.

In the current study, we make inferences about biogeographic history based partly on the phylogeny of 44 sampled species, but also by incorporating the results of other recent studies with much broader taxon sampling (including some with thousands of species; [S42]). First, a large clade including the families Dicroglossidae, Ranidae, Rhacophoridae, and Mantellidae originated within East Asia [S42,S79,S80], and the first three families are represented in our phylogeny by all species descended from the common ancestor of *Nanorana yunnanensis* and *Rhacophorus rhodopus* (figure 1). Hence, microhabitat evolution that occurred after this branching point was ISE within East Asia, which includes terrestriality in *Rhacophorus dugritei* and arboreality in Rhacophoridae (the latter is supported by the fact that Rhacophoridae is nested within a species-rich group of frogs that are almost all semi-aquatic or aquatic; [S21,S42]). Likewise, the Hyloidea likely originated within the Neotropics [S42,S80], which includes Colombia. For example, almost all families of Hyloidea are exclusively Neotropical (or in temperate South America), and the only exceptions are members of two families (Bufonidae, Hylidae), in which the earliest lineages are clearly Neotropical (e.g. [S42,S81]). In our tree, Hyloidea is represented by the common ancestor of *Oreobates quixensis* and Leptodactylidae, Dendrobatidae, Bufonidae, and Hylidae (figure 1; [S42]). Our results suggest that terrestriality

likely arrived in the Neotropics via ECD when hyloids first colonized South America (figure S3), while other microhabitat states clearly originated within the Neotropics through ISE, such as arboreality in Hylidae and semi-aquatic microhabitat use in *Leptodactylus leptodactyloides* (figures 1 and S3). Finally, because Australia was colonized by a presumably arboreal hylid frog (the common ancestor of *Litoria*; figures 1 and S3; [S81]), the other three microhabitat states in this clade (burrowing, terrestrial, and semi-aquatic) must have originated within Australia as ISE. The ancestor of *Litoria* was almost certainly arboreal given that: (i) the sister group to *Litoria* (the Phyllomedusinae) is almost exclusively arboreal, (ii) the sister group to Pelodryadinae + Phyllomedusinae is Hylinae [S42,S81], which is also almost certainly ancestrally arboreal (e.g. species in almost all genera are largely or exclusively arboreal with the exception of the deeply nested terrestrial lineages *Acris* + *Pseudacris* and aquatic lineages *Lysapsus* + *Pseudis*; [S82]); and (iii) previous analyses of microhabitat use within *Litoria* are consistent with the idea that the group is ancestrally arboreal (e.g. the sister group to all other species is a clade of arboreal species; [S4]).

Ecologically conservative dispersal (ECD) occurs through biogeographic dispersal without ecological change. Hylid frogs colonized East Asia while maintaining arboreal microhabitat use [S5,S83], whereas bufonid frogs did so while maintaining terrestrial microhabitat use (figures 1 and S3; [S6]). While the exact biogeographic history of microhylid frogs is uncertain [S8], it is clear that terrestriality evolved in this group before the geographic distribution of its major sub-clades was determined and has not changed in association with biogeographic shifts [S84]. Furthermore, while vicariance due to continental drift has been proposed to explain the distribution of clades of microhylids, neither their divergence dates nor

historical biogeographic patterns are consistent with such a history [S1,S2]. Instead, one dominated by dispersal across continents seems to be the more likely explanation [S8].

We briefly clarify a difference between the scale of ecological and evolutionary processes and our description of ISE and ECD. We note that while our field data come from co-occurring individuals, the species and clades here are not restricted to the sites we sampled and thus character evolution could have happened in another location. In other words, one could imagine that different states (e.g. arboreality, terrestriality) evolved within a region but independently at different local sites, but dispersal within the region would have resulted in the current co-occurrence of these lineages. We emphasize that we are not suggesting that all ISE happened within the specific sites we sampled, but rather within the general region in which our sites occur (i.e. Southeast Asia, Australia, and tropical South America).

Testing for ecologically conservative dispersal in morphology and performance

To examine whether the phenotypic similarity across assemblages is (at least partly) a consequence of dispersal of ecotypes among regions, we first examined three clades of frogs that are found in both China and Colombia and show similar microhabitat use in both places. These clades are Microhylidae (terrestrial; China: *Microhyla fissipes*, Colombia: *Chiasmocleis bassleri* and *Hamptophryne boliviana*), Bufonidae (terrestrial; China: *Duttaphrynus melanostictus*, Colombia: *Rhinella margaritifera* and *Rhinella proboscidea*), and Hylidae (arboreal; China: *Hyla annectans*, Colombia: genera *Dendropsophus*, *Hypsiboas*, *Osteocephalus*, *Scinax*, and *Sphaenorhynchus*).

To see whether ecologically conservative dispersal (ECD) could lead to high similarity among species across locations, we tested whether the species that represented ECD across

continents were very similar in morphology and performance. For each comparison of the Chinese versus Colombian members of the three clades, we first calculated the pairwise Euclidean distance in morphology and performance (separately) between the single species that occurs in China and its closest relative in Colombia (Hylidae) or the mean value of its two equally closest relatives in Colombia (Microhylidae and Bufonidae; see above and figure 1). Given that these distances in PC space are only of use relative to similarly calculated distances among other taxa, we next calculated pairwise distances among all species sharing the same category of microhabitat use (136 and 153 comparisons among terrestrial and arboreal species, respectively), as well as all 209 comparisons of species from China and Colombia. This allowed us to ask, for example: how different are the terrestrial microhylid frogs found in China and Colombia compared to differences among all terrestrial frogs or among all pairs of species from China and Colombia?

Testing for the effects of history and convergent evolution in morphology and performance in an in situ radiation

The Australian hylids (genus *Litoria*) have undergone extensive diversification in microhabitat use (i.e. terrestrial, burrowing, aquatic, arboreal) in ~42 My (crown age; figure 1), whereas their sister group in our phylogeny, the South American hylids, are all arboreal and are ~58.2 My old (crown age; figure 1). Thus, we asked whether this relatively recent diversification in ecology has also resulted in convergent evolution in morphology and performance, given that frogs in similar microhabitat categories around the world cluster in both morphological and performance space (see Results). Conversely, we might expect to see that their prior history of ecological specialization may leave a footprint in their morphology or performance. Specifically, because

688 Australian hylid frogs arrived from South America presumably as arboreal frogs (see above), we
689 might expect that Australian non-arboreal hylids have some aspects of morphology and
690 performance more consistent with arboreality than their current microhabitat use. Or we might
691 find a mixture of both history and convergence – evolution might have been in the direction
692 expected based on convergent evolution, but species in novel microhabitats could still be quite
693 similar to species in the ancestral habitat due to the effects of history [S59,S71].

694 We designed three tests to determine whether a residual effect of history is present, and
695 also whether the amount and direction of evolution in *Litoria* has been consistent with adaptive
696 predictions (i.e. convergence). First, an evolutionary footprint might be seen by species in a
697 novel environment (e.g. terrestrial microhabitat) being closer in morphology and performance to
698 closely related species in the ancestral environment (e.g. arboreal microhabitat) than those
699 species in the ancestral environment are to distantly related species in the new environment.
700 Thus, a simple test of history is to see whether *Litoria* in novel microhabitats are more similar in
701 morphology and performance to arboreal *Litoria* than unrelated species in the novel
702 microhabitats are to arboreal *Litoria*. In other words, due to history *Litoria* in novel
703 microhabitats have not reached the expected outcome of full adaptation to the new microhabitat.

704 Second, if adaptive evolution has led to convergence between *Litoria* in novel
705 microhabitats and other species in those microhabitats, we would expect the distance (in
706 morphology and/or performance) between the *Litoria* using a novel microhabitat (e.g. semi-
707 aquatic) and other frog species using that same microhabitat to be smaller than the distance
708 between these *Litoria* and those in the ancestral microhabitat (arboreal). As in the previous test,
709 distances among these groups in both morphology and performance can easily be calculated and
710 compared.

711 Third, if divergence in *Litoria* were adaptive (whether history were important or not), we
712 would expect that the direction of divergence in non-arboreal *Litoria* would be toward the area of
713 phenotype space occupied by other species using similar microhabitats. A direct test of this
714 prediction is to calculate the correlation between the expected and observed vectors of
715 divergence from an ancestral value. In other words, what proportion of a lineage's observed
716 divergence from its ancestor has been in the direction expected? To assess these possibilities, we
717 can calculate an expected direction and amount of evolution based on the vector (in morphology
718 or performance space) between *Litoria* in the ancestral ecological role and other species of frogs
719 in the novel microhabitat role, as we can consider the mean value of all other species of frogs
720 using a given microhabitat (some for a much longer time period than in *Litoria*), as representing
721 an approximate "optimum" (figure 2; see below for an alternative approach). In statistical terms,
722 this vector could be viewed as the maximum-likelihood path of divergence. Likewise, we can
723 calculate a vector of observed divergence. This is a vector that begins at the mean phenotype of
724 arboreal *Litoria* and ends at the mean value for *Litoria* in the novel microhabitat (figure 2).
725 The correlation between these two vectors [S85] represents the amount of total
726 divergence between the two focal groups that has been in the expected direction of divergence.
727 More formally, the projection of the vector of observed divergence onto the vector of expected
728 divergence is the amount of divergence between arboreal *Litoria* and a given lineage of non-
729 arboreal *Litoria* along the expected trajectory of evolution. This projection (D_{proj}) is simply the
730 cosine of the angle between the two vectors multiplied by the observed amount of divergence
731 ($D_{proj} = D_{obs} \cdot \cos \theta$; figure 2; [S86]). This projection divided by the observed divergence
732 between the two groups of *Litoria* will give the amount of divergence in the expected direction
733 relative to the total observed divergence (D_{proj} / D_{obs}), and this is mathematically equivalent to

734 the vector correlation between the two divergence vectors, as that correlation is the cosine of the
735 angle between the vectors (i.e. $D_{proj} / D_{obs} = (D_{obs} \cdot \cos \theta) / D_{obs} = \cos \theta = r_{vec}$).

736 These three tests allow us to address many questions of convergence and the potential
737 role of history. To carry out these three tests, we first calculated the centroids in morphological
738 and performance space for arboreal *Litoria*, for *Litoria* in each novel microhabitat (i.e. burrowing,
739 semi-aquatic, and terrestrial), and for other species of frogs in our dataset that use the same non-
740 arboreal microhabitat types that have evolved within *Litoria*. We then calculated distances
741 between the centroid for arboreal *Litoria* and *Litoria* in each novel microhabitat (D_{obs}), distances
742 between the latter *Litoria* and the centroid of other frog species in a similar microhabitat (D_{env};
743 for example, semi-aquatic *Litoria* with other semi-aquatic species around the world; figure 2),
744 and distances between arboreal *Litoria* and the centroid of other frog species each novel
745 microhabitat, the expected value based on "complete" convergence (D_{exp}). We note that an
746 alternative approach would be to estimate the phenotypic "optima" in the novel microhabitats by
747 conducting a phylogenetic analysis of character evolution under the Ornstein-Uhlenbeck model
748 [S71,S87], which calculates evolutionary optimal values for discrete selective regimes (in our
749 case, microhabitat). These optimal values are distinct from the current mean values of species in
750 those selective regimes, which may not yet have reached the optima [S71], and they may be
751 better values for calculating the expected divergence between arboreal *Litoria* and those in novel
752 microhabitats. While we focus on the mean values, we also do this latter analysis and find
753 similar results (see below).

754 The test of history was done by comparing the actual divergence between arboreal *Litoria*
755 and those in the novel microhabitat (D_{obs}) and the expected divergence based on other species in
756 the same novel microhabitat (D_{exp}), done individually for each novel microhabitat. The ratio of

these two distances was used as a test statistic (D_{obs} / D_{exp}), where an effect of history would be indicated by values much less than 1. For the distance-based test of convergence, we compared the distance between groups in the same microhabitat to the observed divergence between closely related groups (D_{env} / D_{obs}), with convergence represented by a smaller distance among species in the same microhabitat. This was also used as a test statistic. Finally, we calculated the vector correlation (following [85]) between the vector linking arboreal *Litoria* with *Litoria* in the novel microhabitat (e.g. semi-aquatic) and the vector between arboreal *Litoria* and other species using the same microhabitat as the novel *Litoria* (e.g. semi-aquatic). All these calculations were done separately for each novel microhabitat type.

To test the statistical significance of these quantities, we conducted simulations of phenotypic evolution to produce null distributions against which to test our observed distances and vector correlations. Phenotypic evolution was simulated under Brownian motion because it is a model of neutral evolution [S70,S71] and thus serves as an appropriate null model (i.e. an Ornstein-Uhlenbeck model assumes selection towards phenotypic optima, which is what we are testing here). For these simulations, we first estimated the Brownian motion evolutionary rate matrix [S88] for PC axes across all species in our phylogeny using the "ic.sigma" function in the R package *geiger* [S89]. We next simulated Brownian motion character evolution along the phylogeny using this rate matrix (using the "sim.char" function in *geiger*), and then we calculated distances and vector correlations as above. Because these simulations do not incorporate microhabitat use of species, they produce distances and vector correlations among species that are neutral with respect to adaptive expectations and thus represent null distributions for hypothesis testing. We simulated 9,999 replicates each for morphology and performance.

779 These calculations and simulations allowed us to ask three questions. Note that
780 subsequent statistical tests correspond to these questions in the same order presented here. First,
781 have novel microhabitat specialists in *Litoria* diverged less from the ancestral, arboreal
782 phenotype (as represented by extant arboreal *Litoria*) than expected by convergent evolution (as
783 represented by the distance from arboreal *Litoria* to unrelated species in the novel microhabitat)?
784 Such a lack of "complete" convergence would represent a footprint of evolution history
785 [S59,S71]. Second, are novel microhabitat specialists in *Litoria* more similar to distantly related
786 species in the same microhabitat than to arboreal *Litoria*? If true, we would expect to find that
787 the ratio of distance between groups similar in microhabitat use (D_{env}) and distance between
788 closely related groups (D_{obs}) to be small. Third, has the direction of divergence of *Litoria* in
789 novel microhabitats from the ancestral phenotype been primarily toward the mean phenotype of
790 other species in the same (novel) microhabitat? This would be shown by finding a high vector
791 correlation, with values close to 1 showing the strongest support (e.g. $r_{vec} = 1$ would mean all
792 observed divergence was in the direction expected).
793 Statistical significance was assessed with these simulations in two ways. First, we
794 examined each microhabitat transition in *Litoria* individually (i.e. for burrowing, semi-aquatic,
795 and terrestrial *Litoria*) by asking: (i) in what proportion of simulation replicates was the ratio of
796 expected divergence between arboreal *Litoria* and unrelated species in the novel microhabitat to
797 observed divergence among *Litoria* (D_{exp} / D_{obs}) smaller than our empirical results, (ii) in what
798 proportion of simulation replicates was the ratio of the distance between species in similar
799 microhabitats to observed distance (D_{env} / D_{obs}) smaller than our empirical results, and (iii) in
800 what proportion of simulations was the vector correlation greater (closer to 1) than the observed
801 correlation?

802 Second, to assess more generally whether morphological and performance evolution in
803 *Litoria* has been consistent with adaptive predictions across all microhabitat transitions, we also
804 calculated: (i) the proportion of simulation replicates in which all three random distance ratios
805 were smaller than all three observed ratios (i.e. for all three microhabitat categories) for this
806 history test, (ii) the same quantity for the distance-based convergence test, and (iii) the
807 proportion of simulation replicates in which all three vector correlations were larger than all
808 three observed correlations. For example, if a given random simulation produced a vector
809 correlation that was larger than observed for burrowing *Litoria* but not for semi-aquatic and
810 terrestrial *Litoria*, this correlation was not considered as extreme as the observed set of
811 correlations that we would expect by chance.
812 As mentioned above, one could alternatively estimate the expected convergent
813 phenotypes by using a comparative analysis of adaptation to discrete selective regimes (as in
814 microhabitats here), using the approach of Hansen [S71] and Butler and King [S87]. Thus, we
815 tested the robustness of our results using mean values of extant species to those using these OU
816 optima. To do this, we first estimated ancestral states of microhabitat use at internal nodes. This
817 was done using the likelihood method of Schluter et al. [S90] in the R package *diversitree* [S91].
818 We estimated ancestral states under a model of unordered, equal transition rates among all states,
819 which was the model with the highest support among those commonly tested (equal rates: AIC =
820 92.9; symmetric: AIC = 101.3; all rates different: AIC = 121.3). Given that most current
821 implementations of OU models necessitate specifying single states at internal nodes, for each
822 node we chose the state that had the highest proportional likelihood. In most cases one state had
823 the highest support by far (figure S3), though the two nodes in the Myobatrachidae gave roughly
824 equal support for terrestriality and burrowing. We ran OU analyses assuming each of the two

825 possibilities (for four possible combinations) but found roughly similar OU optima, so we
826 present results only from the ML estimates at these nodes (i.e. both terrestrial).
827 We ran OU models with the R package OUCH [S87] assuming each PC axis was
828 independent. We recognize that these axes are not independent in an OU analysis (i.e. the PCA
829 was done assuming Brownian motion as the model of non-independence among taxa). However,
830 multivariate OU approaches that accommodate trait non-independence involved many more
831 parameters and seemed to become trapped on local optima (e.g. the likelihood of more complex
832 models was lower than for simpler models). For both performance and morphology, we first
833 tested three possible models: (i) Brownian motion, (ii) OU with a single optimum for all species,
834 and (iii) OU with four separate optima corresponding to our four microhabitat categories.
835 Because PC axes were assumed to be independent, we added the likelihoods of all PC axes
836 together to obtain the overall likelihood of each model across all traits, done separately for
837 morphology and performance. Finally, we conducted these analyses without the 11 species of
838 *Litoria* so as to estimate the optimal morphology and performance of microhabitats (i.e. the
839 optimum toward which novel-microhabitat *Litoria* may have diverged from the ancestral
840 arboreal morphology and performance).
841 As expected based on our previous MANOVA, we found that the microhabitat-specific
842 model had the lowest AIC for both morphology and performance (morphology: Brownian
843 motion AIC = 1276, single-optimum OU AIC = 1271, microhabitat-based OU AIC = 1200;
844 performance: Brownian motion AIC = 1227, single-optimum OU AIC = 1219, microhabitat-
845 based OU AIC = 1206). Thus, we used the estimated optimum value of each PC axis for each
846 microhabitat from this analysis in place of the non-*Litoria* microhabitat means (for burrowing,
847 semi-aquatic, and terrestrial) for the above tests of history and convergence. Our results for the

history and convergence analyses when using the OU optima were qualitatively identical. This was because the OU optima were nearly quantitatively identical to the extant species means (morphology: burrowing $r_{vec} = 0.982$, semi-aquatic $r_{vec} = 0.965$, terrestrial $r_{vec} = 0.993$; performance: burrowing $r_{vec} = 0.975$, semi-aquatic $r_{vec} = 0.977$, terrestrial $r_{vec} = 0.967$).

References

S1. Roelants K, Gower DJ, Wilkinson M, Loader SP, Biju SD, Guillaume K, Moriau L, Bossuyt F. 2007 Global patterns of diversification in the history of modern amphibians. *Proc. Nat. Acad. Sci. USA* **104**, 887–892. (doi:10.1073/pnas.0608378104)

S2. Wiens JJ. 2007 Global patterns of species richness and diversification in amphibians. *Am. Nat.* **170**, S86–S106. (doi:10.1086/519396)

S3. AmphibiaWeb. 2012 *AmphibiaWeb: Information on amphibian biology and conservation* Berkeley, CA, USA. <http://amphibiaweb.org/>. Accessed on 30 August 2012.

S4. Young JE, Christian KA, Donnellan S, Tracy CR, Parry D. 2005 Comparative analysis of cutaneous evaporative water loss in frogs demonstrates correlation with ecological habits. *Physiol. Biochem. Zool.* **78**, 847–856. (doi:10.1086/432152)

S5. Smith SA, Stephens PR, Wiens JJ. 2005 Replicate patterns of species richness, historical biogeography, and phylogeny in Holarctic treefrogs. *Evolution* **59**, 2433–2450.

S6. Van Bocxlaer I, Loader SP, Roelants K, Biju SD, Menegon M, Bossuyt F. 2010 Gradual adaptation toward a range-expansion phenotype initiated the global radiation of toads. *Science* **327**, 679–682. (doi:10.1126/science.1181707)

S7. Wiens JJ, Sukumaran J, Pyron RA, Brown RM. 2009 Evolutionary and biogeographic origins of high tropical diversity in Old World frogs (Ranidae). *Evolution* **63**, 1217–1231. (doi:10.1111/j.1558-5646.2009.00610.x)

S8. van der Meijden A, Vences M, Hoegg S, Boistel R, Channing A, Meyer, A. 2007 Nuclear gene phylogeny of narrow-mouthed toads (Family: Microhylidae) and a discussion of competing hypothesis concerning their biogeographical origins. *Mol. Phylogenet. Evol.* **44**, 1017–1030. (doi:10.1016/j.ympev.2007.02.008)

S9. Lynch JD. 2005 Discovery of the richest frog fauna in the World – an exploration of the forests to the north of Leticia. *Rev. Acad. Colomb. Cienc.* **29**, 581–588.

S10. Yang DT, Rao DQ. 2008 *Amphibia and Reptilia of Yunnan*. Kunming, China: Yunnan Publishing Group Corporation - Yunnan Science and Technology Press.

S11. Kuo C-Y, Gillis GB, Irschick DJ. 2011 Loading effects on jump performance in green anole lizards, *Anolis carolinensis*. *J. Exp. Biol.* **214**, 2073–2079. (doi:10.1242/jeb.053355)

S12. Gans C, Parsons TS. 1966 On the origin of jumping mechanism in frogs. *Evolution* **20**, 92–99.

S13. Zug GR. 1978 Anuran locomotion – structure and function. 2. Jumping performance of semiaquatic, terrestrial, and arboreal frogs. *Smiths. Contrib. Zool.* **276**, 1–31.

S14. Emerson SB. 1979 The ilio-sacral articulation in frogs: form and function. *Biol. J. Linn. Soc.* **11**, 153–168.

S15. Emerson SB. 1982 Frog postcranial morphology: identification of a functional complex. *Copeia* **3**, 603–613.

890 S16. Nauwelaerts S, Ramsay J, Aerts P. 2007 Morphological correlates of aquatic and
891 terrestrial locomotion in a semi-aquatic frog, *Rana esculenta*: no evidence for a design
892 conflict. *J. Anat.* **210**, 304–317. (doi:10.1111/j.1469-7580.2007.00691.x)
893 S17. Emerson S, Diehl D. 1980 Toe pad morphology and mechanisms of sticking in frogs.
894 *Biol. J. Linn. Soc.* **13**, 199–216.
895 S18. Emerson SB. 1991 The ecomorphology of Bornean tree frogs (family Rhacophoridae).
896 *Zool. J. Linn. Soc.* **101**, 337–357.
897 S19. Taigen TL, Emerson SB, Pough FH. 1982 Ecological correlates of anuran exercise
898 physiology. *Oecologia* **52**, 49–56.
899 S20. Taigen TL, Pough FH. 1985 Metabolic correlates of anuran behavior. *Am. Zool.* **25**, 987–
900 997.
901 S21. Duellman WE, Trueb L. 1986 *Biology of Amphibians.* Baltimore, MD: Johns Hopkins
902 University Press.
903 S22. Bennett AF, Licht P. 1973 Relative contributions of anaerobic and aerobic energy
904 production during activity in Amphibia. *J. Comp. Physiol.* **87**, 351–360.
905 S23. Bennett AF, Licht P. 1974 Anaerobic metabolism during activity in amphibians. *Comp.*
906 *Biochem. Physiol.* **48A**, 319–327.
907 S24. Walker JA. 1998 Estimating velocities and accelerations of animal locomotion: a
908 simulation experiment comparing numerical differentiation algorithms. *J. Exp. Biol.* **201**,
909 981–995.
910 S25. Marsh RL. 1994 Jumping ability of anuran amphibians. In *Advances in Veterinary*
911 *Science and Comparative Medicine, Vol. 38B* (ed. Jones JH), pp. 51–111. New York, NY,
912 USA: Academic Press.

913 S26. Navas CA, Gomes FR, Carvalho JE. 2008 Thermal relationships and exercise physiology
914 in anuran amphibians: integration and evolutionary implications. *Comp. Biochem.*
915 *Physiol. A* **151**, 344–362. (doi:10.1016/j.cbpa.2007.07.003)
916 S27. Hirano M, Rome LC. 1984 Jumping performance of frogs (*Rana pipiens*) as a function of
917 muscle temperature. *J. Exp. Biol.* **108**, 429–439.
918 S28. James RS, Navas CA, Herrel A. 2007 How important are skeletal muscle mechanics in
919 setting limits on jumping performance? *J. Exp. Biol.* **210**, 923–933.
920 S29. Burton Z, Bhushan B. 2006 Surface characterization and adhesion and friction properties
921 of hydrophobic leaf surfaces. *Ultramicroscopy* **106**, 709–719.
922 S30. Walker JS. 2004 *Physics,* 2nd Ed. Upper Saddle River, NJ, USA: Pearson Education.
923 S31. Bikerman J. 1971 Theory of adhesive joints. In *Adhesion and Bonding* (ed. Bikales NM),
924 pp. 35–40. New York, NY, USA: Wiley.
925 S32. Rasband WS. 1997 *ImageJ.* Bethesda, MD, USA: U. S. National Institutes of Health.
926 <http://imagej.nih.gov/ij/>.
927 S33. Woltring HJ. 1985 On optimal smoothing and derivative estimation from noisy
928 displacement data in biomechanics. *Hum. Movmt. Sci.* **4**, 229–245.
929 S34. Marsh RL, John-Alder HB. 1994 Jumping performance of hylid frogs measured with
930 high-speed cine film. *J. Exp. Biol.* **188**, 131–141.
931 S35. James RS, Wilson RS. 2008 Explosive jumping: extreme morphological and
932 physiological specializations of Australian rocket frogs (*Litoria nasuta*). *Physiol.*
933 *Biochem. Zool.* **81**, 176–185. (doi:10.1086/525290)

934 S36. Toro E, Herrel A, Irschick DJ. 2003 A biomechanical analysis of intra- and interspecific
935 scaling of jumping and morphology in Caribbean *Anolis* lizards. *J. Exp. Biol.* **206**, 2641–
936 2652. (doi:10.1242/jeb.00473)
937 S37. Emerson SB. 1976 Burrowing in frogs. *J. Morphol.* **149**, 437–458.
938 S38. Lee JC. 1982 Accuracy and precision in anuran morphometrics: artifacts of preservation.
939 *Syst. Zool.* **31**, 266–281.
940 S39. Deichmann JL, Boundy J, Williamson GB. 2009 Anuran artifacts of preservation: 27
941 years later. *Phyllomedusa* **8**, 51–58.
942 S40. Heyer WR. 1969 The adaptive ecology of the species groups of the genus *Leptodactylus*
943 (Amphibia, Leptodactylidae). *Evolution* **23**, 421–428.
944 S41. Ponssa ML, Barrionuevo JS. 2012 Sexual dimorphism in *Leptodactylus latinasus* (Anura,
945 Leptodactylidae): nasal capsule anatomy, morphometric characters and performance
946 associated with burrowing behavior. *Acta Zool. – Stockholm* **93**, 57–67.
947 (doi:10.1111/j.1463-6395.2010.00479.x)
948 S42. Pyron RA, Wiens JJ. 2011 A large-scale phylogeny of Amphibia including over 2800
949 species, and a revised classification of extant frogs, salamanders, and caecilians. *Mol.*
950 *Phylogenet. Evol.* **61**, 543–583. (doi:10.1016/j.ympev.2011.06.012)
951 S43. Drummond AJ, Ho SYW, Phillips MJ, Rambaut A. 2006 Relaxed phylogenetics and
952 dating with confidence. *PLoS Biol.* **4**, e88. (doi:10.1371/journal.pbio.0040088)
953 S44. Drummond A, Rambaut A. 2007 BEAST: Bayesian evolutionary analysis by sampling
954 trees. *BMC Evol. Biol.* **7**, 214–221. (doi:10.1186/1471-2148-7-214)
955 S45. Wiens JJ, Morrill MC. 2011 Missing data in phylogenetic analysis: reconciling results
956 from simulations and empirical data. *Syst. Biol.* **60**, 719–731. (doi:10.1093/sysbio/syr025)

957 S46. Fei L, Hu SQ, Ye CY, Huang YZ. 2009 *Fauna Sinica, Amphibia*. *Vol. 3, Anura, Ranidae.*
958 Beijing, China: Chinese Academic Science Press.
959 S47. Frost DR. 2011 *Amphibian Species of the World: an Online Reference. Version 5.5*. New
960 York, NY, USA: American Museum of Natural History.
961 <http://research.amnh.org/vz/herpetology/amphibia/>
962 S48. Wiens JJ. 2011 Re-evolution of lost mandibular teeth in frogs after more than 200 million
963 years, and re-evaluating Dollo's law. *Evolution* **65**, 1283–1296. (doi:10.1111/j.1558-
964 5646.2011.01221.x)
965 S49. Jolicoeur P. 1963 The multivariate generalization of the allometry equation. *Biometrics*
966 **19**, 497–499.
967 S50. Moen DS, Smith SA, Wiens JJ. 2009 Community assembly through evolutionary
968 diversification and dispersal in Middle American treefrogs. *Evolution* **63**, 3228–3247.
969 (doi:10.1111/j.1558-5646.2009.00810.x)
970 S51. Emerson SB. 1978 Allometry and jumping in frogs: helping the Twain to meet. *Evolution*
971 **32**, 551–564.
972 S52. Wilson RS, Franklin CE, James RS. 2000 Allometric scaling relationships of jumping
973 performance in the striped marsh frog *Limnodynastes peronii*. *J. Exp. Biol.* **203**, 1937–
974 1946.
975 S53. Manly BFJ. 1994 *Multivariate Statistical Methods: a Primer*. London: Chapman and Hall.
976 S54. Revell LJ. 2009 Size-correction and principal components for interspecific comparative
977 studies. *Evolution* **63**, 3258–3268. (doi:10.1111/j.1558-5646.2009.00804.x)

978 S55. R Development Core Team. 2012 *R: A Language and Environment for Statistical*
979 *Computing*. Vienna, Austria: R Foundation for Statistical Computing. ISBN 3-900051-
980 07-0, URL <http://www.R-project.org/>
981 S56. Revell LJ. 2012 phytools: an R package for phylogenetic comparative biology (and other
982 things). *Methods Ecol. Evol.* **3**, 217–223. (doi:10.1111/j.2041-210X.2011.00169.x)
983 S57. Franklin S, Gibson D, Robertson P, Pohlmann J, Fralish J. 1995 Parallel Analysis: a
984 method for determining significant components. *J. Vegetat. Sci.* **1995**, 99–106.
985 S58. Winemiller KO. 1991 Ecomorphological diversification in lowland freshwater fish
986 assemblages from five biotic regions. *Ecol. Mono.* **61**, 343–365.
987 S59. Stayton CT. 2006 Testing hypotheses of convergence with multivariate data:
988 morphological and functional convergence among herbivorous lizards. *Evolution* **60**,
989 824–841. (doi:10.1554/04-575.1)
990 S60. Revell LJ, Johnson MA, Schulte II JA, Kolbe JJ, Losos JB. 2007 A phylogenetic test for
991 convergence in rock-dwelling lizards. *Evolution* **61**, 2898–2912. (doi:10.1111/j.1558-
992 5646.2007.00225.x)
993 S61. Arnold SJ. 1983 Morphology, performance and fitness. *Am. Zool.* **23**, 347–361.
994 S62. Wainwright PC. 1991 Ecological morphology: experimental functional anatomy for
995 ecological problems. *Am. Zool.* **31**, 680–693.
996 S63. Irschick DJ, Meyers JJ, Husak JF, Le Galliard JF. 2008 How does selection operate on
997 whole-organism functional performance capacities? A review and synthesis. *Evol. Ecol.*
998 *Res.* **10**, 177–196.
999 S64. Koehl MAR. 1996 When does morphology matter? *Ann. Rev. Ecol. Syst.* **27**, 501–542.

1000 S65. Wainwright PC, Alfaro ME, Bolnick DI, Hulsey CD. 2005 Many-to-one mapping of
1001 form to function: a general principle in organismal design? *Integr. Comp. Biol.* **45**, 256–
1002 262.
1003 S66. Vanhooydonck B, Herrel A, Van R Damme, Irschick D. 2006 The quick and the fast: the
1004 evolution of acceleration capacity in *Anolis* lizards. *Evolution* **60**, 2137–2147.
1005 (doi:10.1111/j.0014-3820.2006.tb01851.x)
1006 S67. Collar DC, Wainwright PC. 2006 Discordance between morphological and mechanical
1007 diversity in the feeding mechanism of centrarchid fishes. *Evolution* **60**, 2575–2584.
1008 (doi:10.1111/j.0014-3820.2006.tb01891.x)
1009 S68. Wainwright PC. 2007 Functional versus morphological diversity in macroevolution. *Ann.*
1010 *Rev. Ecol. Evol. Syst.* **38**, 381–401. (doi:10.1146/annurev.ecolsys.38.091206.095706)
1011 S69. Martins EP, Hansen TF. 1997 Phylogenies and the comparative method: a general
1012 approach to incorporating phylogenetic information into the analysis of interspecific data.
1013 *Am. Nat.* **149**, 646–667.
1014 S70. Felsenstein J. 1988 Phylogenies and quantitative characters. *Ann. Rev. Ecol. Syst.* **19**,
1015 445–471.
1016 S71. Hansen TF. 1997 Stabilizing selection and the comparative analysis of adaptation.
1017 *Evolution* **51**, 1341–1351.
1018 S72. Rohlf FJ, Corti M. 2000 Use of two-block partial least-squares to study covariation in
1019 shape. *Syst. Biol.* **49**, 740–753.
1020 S73. Jackson JE. 1991 *A User's Guide to Principal Components Analysis*. New York: John
1021 Wiley and Sons.

1022 S74. Pagel M. 1993 Seeking the evolutionary regression coefficient: an analysis of what
1023 comparative methods measure. *J. Theor. Biol.* **164**, 191–205.
1024 S75. Rohlf FJ. 2006 A comment on phylogenetic correction. *Evolution* **60**, 1509–1515.
1025 S76. Todorov V, Filzmoser P. 2009 An object oriented framework for robust multivariate
1026 analysis. *J. Stat. Soft.* **32**, 1–47.
1027 S77. Blankers T, Adams DC, Wiens JJ. 2012 Ecological radiation with limited morphological
1028 diversification in salamanders. *J. Evol. Biol.* **25**, 634–646. (doi:10.1111/j.1420-
1029 9101.2012.02458.x)
1030 S78. Stephens PR, Wiens JJ. 2004 Convergence, divergence, and homogenization in the
1031 ecological structure of emydid turtle communities: the effects of phylogeny and dispersal.
1032 *Am. Nat.* **164**, 244–254. (doi:10.1086/422342)
1033 S79. Bossuyt F, Brown RM, Hillis DM, Cannatella DC, Milinkovitch MC. 2006 Phylogeny
1034 and biogeography of a cosmopolitan frog radiation: late Cretaceous diversification
1035 resulted in continent-scale endemism in the family Ranidae. *Syst. Biol.* **55**, 579–594.
1036 (doi:10.1080/10635150600812551)
1037 S80. Darst CR, Cannatella DC. 2004 Novel relationships among hyloid frogs inferred from
1038 12S and 16S mitochondrial DNA sequences. *Mol. Phylogenet. Evol.* **31**, 462–475.
1039 (doi:10.1016/j.ympev.2003.09.003)
1040 S81. Wiens JJ, Pyron RA, Moen DS. 2011 Phylogenetic origins of local-scale diversity
1041 patterns and causes of Amazonian megadiversity. *Ecol. Lett.* **14**, 643–652.
1042 (doi:10.1111/j.1461-0248.2011.01625.x)
1043 S82. Duellman WE. 2001 *The Hylid Frogs of Middle America*, 2nd Ed. Lawrence, KS, USA:
1044 Society for the Study of Amphibians and Reptiles.

1045 S83. Wiens JJ. 2011 The niche, biogeography and species interactions. *Phil. Trans. R. Soc. B*
1046 **366**, 2336–2350. (doi:10.1098/rstb.2011.0059)
1047 S84. Vitt LJ, Caldwell JP. 2009 *Herpetology*, 3rd Ed. Burlington, MA, USA: Academic Press.
1048 S85. Collyer ML, Adams DC. 2007 Analysis of two-state multivariate phenotypic change in
1049 ecological studies. *Ecology* **88**, 683–692. (doi:10.1890/06-0727)
1050 S86. Hansen TF, Houle D. 2008 Measuring and comparing evolvability and constraint in
1051 multivariate characters. *J. Evol. Biol.* **21**, 1201–1219. (doi:10.1111/j.1420-
1052 9101.2008.01573.x)
1053 S87. Butler MA, King AA. 2004 Phylogenetic comparative analysis: a modeling approach for
1054 adaptive evolution. *Am. Nat.* **164**, 683–695.
1055 S88. Revell LJ, Harmon LJ, Langerhans RB, Kolbe JJ. 2007 A phylogenetic approach to
1056 determining the importance of constraint on phenotypic evolution in the neotropical
1057 lizard, *Anolis cristatellus*. *Evol. Ecol. Res.* **9**, 261–282.
1058 S89. Harmon L, Weir J, Brock C, Glor R, Challenger W, Hunt G. 2009 *geiger: Analysis of*
1059 *Evolutionary Diversification*. R package version 1.3-1. <http://CRAN.R-
1060 project.org/package=geiger>
1061 S90. Schluter D, Price T, Mooers AO, Ludwig D. 1997 Likelihood of ancestor states in
1062 adaptive radiation. *Evolution* **51**, 1699–1711.
1063 S91. FitzJohn RG. 2012 Diversitree: comparative phylogenetic analyses of diversification in R.
1064 *Methods Ecol. Evol.* **3**, 1084–1092. (doi:10.1111/j.2041-210X.2012.00234.x)
1065 S92. Hero JM, Roberts D, Horner P, Retallick R, Parker F, Iskandar D. 2004 *Limnodynastes*
1066 *convexiusculus*. IUCN Red List of Threatened Species. Version 2011.2.
1067 <www.iucnredlist.org>. Downloaded on 25 May 2012.

1068 S93. Tyler MJ, Smith LA, Johnstone RE. 2000 *Frogs of Western Australia*. Perth, Western
1069 Australi: Western Australia Museum.
1070 S94. Hero JM, Clarke J, Meyer E, Robertson P, Lemckert F, Roberts D, Horner P. 2004
1071 *Platyplectrum ornatum*. IUCN Red List of Threatened Species. Version 2011.2.
1072 <www.iucnredlist.org>. Downloaded on 25 May 2012.
1073 S95. Tyler MJ, Davies M, Martin AA. 1981 Australian frogs of the leptodactylid genus
1074 *Uperoleia* Gray. *Aust. J. Zool. Supp. Ser.* **79**, 1–64.
1075 S96. Liu WZ, Yang DT. 2000 A new species of *Amolops* (Anura: Ranidae) from Yunnan,
1076 China, with a discussion of karyological diversity in *Amolops*. *Herpetologica* **56**, 231–
1077 238.
1078 S97. Chanda SK. 2002 *Hand Book - Indian Amphibians*. Calcutta, India: published by the
1079 Director, Zoological Survey of India.
1080 S98. IUCN Red List of Threatened Species. Version 2011.2. <www.iucnredlist.org>.
1081 Downloaded on 25 May 2012.
1082 S99. Ahmed MF, Das A, Dutta SK. 2009 *Amphibians and Reptiles of Northeast India - a*
1083 *Photographic Guide*. Guwahati, India: Aaranyak.
1084 S100. Inger RF, Zhao EM, Shaffer HB, Wu G. 1990 Report on a collection of amphibians and
1085 reptiles from Sichuan, China. *Fieldiana Zool. NS* **58**, 1–24.
1086 S101. Yang DT, Lu S, Ohler A, Swan S. 2004 *Odorrana grahami*. IUCN Red List of
1087 Threatened Species. Version 2011.2. <www.iucnredlist.org>. Downloaded on 25 May
1088 2012.
1089 S102. Inger RF, Orlov N, Darevsky IS. 1999 Frogs of Vietnam: a report on new collections.
1090 *Fieldiana Zool.* **92**, 1–46.

S103. Duellman WE. 2005 *Cusco Amazónico.* Ithaca, NY, USA: Comstock Publishing Associates, Cornell University Press.

S104. Rodríguez LO, Duellman WE. 1994 *Guide to the Frogs of the Iquitos Region, Amazonian Perú*. Lawrence, Kansas, USA: Asociación de Ecología y Conservación, Amazon Center for Environmental Education and Research, and the Natural History Museum, University of Kansas.

S105. Duellman WE. 1978 The biology of an equatorial herpetofauna in Amazonian Ecuador. *Misc. Pub. Univ. Kansas Mus. Nat. Hist.* **65**, 1–352.

S106. Cochran DM, Goin CJ. 1970 *Frogs of Colombia*. Washington, DC, USA: United States National Museum Bulletin, Smithsonian Institution Press.

Table S1. Species used in this study and classification of microhabitat use. Definition of microhabitat use categories is described in *Material and Methods*. Family names follow assignment by Pyron and Wiens [S42]. Generic taxonomy follows AmphibiaWeb [S3]. References are for microhabitat use. In cases where another species was used to determine microhabitat use, that species has at some point in the past been classified as synonymous with the species of this study; hence, we do not expect its microhabitat use to be different (i.e. lack of distinctive morphological and ecological differences was the reason for past synonymy). Sources for *Amolops tuberodepressus* and *Odorrana grahami* only indicate that these species are found near fast-flowing streams. When collecting these two species in the field, we always found them perched on vegetation above the streams and thus we classify them as arboreal. Information on microhabitat use is largely absent for *Calluella yunnanensis*. However, IUCN [S98] indicates burrowing as characteristic for almost all other members of the genus, so we extend that characterization to *C. yunnanensis*.

Location	Species	Family	Microhabitat use	Reference
Fogg Dam, NT, Australia				
	Limnodynastes convexiusculus	Myobatrachidae	Terrestrial	S92
	Litoria australis	Hylidae	Burrowing	S93
	Litoria bicolor	Hylidae	Arboreal	S93
	Litoria caerulea	Hylidae	Arboreal	S93
	Litoria dahlii	Hylidae	Semi-aquatic	S93
	Litoria inermis	Hylidae	Terrestrial	S93
	Litoria longipes	Hylidae	Burrowing	S93
	Litoria nasuta	Hylidae	Terrestrial	S93
	Litoria pallida	Hylidae	Terrestrial	S93
	Litoria rothii	Hylidae	Arboreal	S93
	Litoria rubella	Hylidae	Arboreal	S93
	Litoria tornieri	Hylidae	Terrestrial	S93
	Platyplectrum ornatum	Myobatrachidae	Burrowing	S94
	Uperoleia lithomoda	Myobatrachidae	Burrowing	S95
Baoshan, Yunnan, China				
	Amolops tuberodepressus	Ranidae	Arboreal	S96

Calluella yunnanensis	Microhylidae	Burrowing	S98
Chiromantis doriae	Rhacophoridae	Arboreal	S97
Hyla annectans	Hylidae	Arboreal	S99
Microhyla fissipes	Microhylidae	Terrestrial	S97 (as *M. ornata*)
Nanorana yunnanensis	Dicroglossidae	Semi-aquatic	S100
Odorrana grahami	Ranidae	Arboreal	S101
Rhacophorus dugritei	Rhacophoridae	Terrestrial	S100
Rhacophorus rhodopus	Rhacophoridae	Arboreal	S102 (as *R. bipunctatus*)
Leticia, Amazonas, Colombia			
Adenomera hylaedactyla	Leptodactylidae	Terrestrial	S103
Allobates femoralis	Dendrobatidae	Terrestrial	S103
Ameerega trivittata	Dendrobatidae	Terrestrial	S104
Chiasmocleis bassleri	Microhylidae	Terrestrial	S105
Dendropsophus rhodopeplus	Hylidae	Arboreal	S103
Dendropsophus sarayacuensis	Hylidae	Arboreal	S105
Dendropsophus triangulum	Hylidae	Arboreal	S105
Hamptophyrne boliviana	Microhylidae	Terrestrial	S103
Hypsiboas hobbsi	Hylidae	Arboreal	S106
Hypsiboas lanciformis	Hylidae	Arboreal	S105
Hypsiboas punctatus	Hylidae	Arboreal	S103
Leptodactylus leptodactyloides	Leptodactylidae	Semi-aquatic	S103
Leptodactylus rhodomystax	Leptodactylidae	Terrestrial	S104
Oreobates quixensis	Craugastoridae	Terrestrial	S105
Osteocephalus planiceps	Hylidae	Arboreal	S103
Rhinella margaritifera	Bufonidae	Terrestrial	S103 (as *Bufo typhonius*)
Rhinella proboscidea	Bufonidae	Terrestrial	S103 (as *Bufo typhonius*)
Scinax ruber	Hylidae	Arboreal	S103
Sphaenorhynchus lacteus	Hylidae	Arboreal	S103

Table S2. Performance data (species mean ± 1 standard error).

Location	Species	Jumping performance				
		n	Peak velocity (m/s)	Peak acceleration (m/s^2)	Peak power (W/kg)	Angle (º)
Fogg Dam, NT, Australia						
	Limnodynastes convexiusculus	5	2.11±0.08	60.82±4.20	78.56±5.82	37.00±2.20
	Litoria australis	6	2.66±0.09	50.19±2.10	99.04±7.70	40.21±6.86
	Litoria bicolor	7	2.61±0.09	96.36±5.17	181.63±19.20	35.78±3.97
	Litoria caerulea	6	2.55±0.11	39.42±3.48	71.97±9.03	45.12±3.61
	Litoria dahlii	8	2.61±0.07	62.53±3.69	112.63±10.45	41.23±4.99
	Litoria inermis	1	2.74	85.36	163.83	38.87
	Litoria longipes	6	2.07±0.09	57.06±4.62	79.12±8.11	33.51±3.49
	Litoria nasuta	7	3.87±0.12	137.91±7.01	367.81±39.84	47.38±2.45
	Litoria pallida	2	3.58±0.57	120.08±23.37	295.17±101.44	44.42±3.21
	Litoria rothii	6	3.36±0.11	90.20±6.41	213.83±15.90	48.48±6.14
	Litoria rubella	6	2.13±0.05	69.83±3.22	101.00±7.20	39.95±4.76
	Litoria tornieri	8	3.14±0.07	123.03±5.14	255.55±14.51	43.15±2.57
	Platyplectrum ornatum	6	2.12±0.09	81.52±6.02	111.89±13.34	47.87±4.81
	Uperoleia lithomoda	3	1.21±0.06	50.03±1.76	32.98±3.12	35.91±3.26
Baoshan, Yunnan, China						
	Amolops tuberodepressus	5	2.32±0.15	55.48±6.05	79.14±2.74	26.64±5.48
	Babina pleuraden	6	2.65±0.05	76.46±3.80	120.35±6.74	42.39±2.45
	Calluella yunnanensis	1	1.98	71.17	89.95	35.03
	Chiromantis doriae	5	2.14±0.07	67.80±6.29	94.97±10.83	29.21±4.57
	Duttaphrynus melanostictus	3	1.10±0.20	20.69±6.45	15.63±5.85	32.21±3.34
	Hyla annectans	5	1.81±0.06	47.03±3.73	57.80±8.82	32.78±2.24
	Microhyla fissipes	5	2.51±0.19	108.23±2.21	175.95±15.69	47.28±3.21
	Nanorana yunnanensis	1	2.68	57.07	98.28	32.93

Odorrana grahami	6	3.37±0.12	73.68±2.09	148.16±7.15	31.10±2.07
Rhacophorus dugritei	5	1.73±0.03	35.59±2.38	41.92±2.37	21.52±1.57
Rhacophorus rhodopus	6	2.02±0.13	43.02±2.86	64.68±6.98	38.28±4.62
Leticia, Amazonas, Colombia					
Adenomera hylaedactyla	5	2.10±0.09	90.08±3.82	121.35±4.86	39.52±7.33
Allobates femoralis	1	2.26	114.54	168.16	37.86
Ameerega trivittata	2	2.12±0.29	59.60±16.86	86.30±28.71	38.38±1.32
Chiasmocleis bassleri	5	1.97±0.04	80.78±3.95	108.62±5.79	35.80±2.89
Dendropsophus rhodopeplus	1	2.54	98.05	169.77	33.10
Dendropsophus sarayacuensis	7	2.96±0.14	124.14±8.85	251.90±30.72	44.29±1.74
Dendropsophus triangulum	7	2.63±0.09	101.10±3.15	178.95±10.20	33.26±3.66
Hamptophryne boliviana	3	1.95±0.07	82.51±7.28	102.35±13.35	42.13±8.32
Hypsiboas hobbsi	7	2.43±0.07	60.76±3.90	104.37±8.26	34.59±2.93
Hypsiboas lanciformis	8	3.35±0.09	64.57±3.89	148.58±7.93	37.11±3.12
Hypsiboas punctatus	7	2.30±0.08	54.85±5.68	79.23±10.87	30.27±1.41
Leptodactylus leptodactyloides	7	2.38±0.10	91.12±10.41	142.45±21.31	37.91±3.24
Leptodactylus rhodomystax	8	2.49±0.05	56.16±2.83	91.26±4.89	34.95±2.72
Oreobates quixensis	4	2.72±0.09	78.83±6.02	137.43±11.83	34.95±1.73
Osteocephalus planiceps	6	3.61±0.10	84.23±9.27	219.74±23.00	33.62±3.20
Rhinella margaritifera	7	1.72±0.06	35.18±1.98	38.04±2.36	38.95±2.39
Rhinella proboscidea	2	1.34±0.10	28.06±1.06	23.61±2.20	37.59±13.94
Scinax ruber	6	2.72±0.09	92.82±3.09	169.74±6.20	30.64±1.91
Sphaenorhynchus lacteus	1	2.47	61.04	107.58	28.46

Location	Species	Swimming performance				Clinging performance	
		n	Peak velocity (m/s)	Peak acceleration (m/s^2)	Peak power (W/kg)	*n*	Maximum angle (º)
Fogg Dam, NT, Australia							
	Limnodynastes convexiusculus	5	0.82±0.04	23.71±3.28	12.88±1.79	5	84.2±9.66
	Litoria australis	6	1.12±0.07	25.19±2.00	18.74±2.24	6	59.0±2.86
	Litoria bicolor	7	1.29±0.03	42.46±4.22	37.29±4.05	7	180.0±0.00
	Litoria caerulea	6	0.97±0.06	19.66±1.96	12.61±1.71	6	146.3±8.47
	Litoria dahlii	8	1.73±0.10	44.97±4.21	52.71±7.70	8	65.4±3.71
	Litoria inermis	1	1.20	53.80	39.32	1	127.0
	Litoria longipes	6	0.75±0.06	18.43±3.20	9.59±2.30	6	79.3±8.64
	Litoria nasuta	7	1.78±0.07	45.99±3.75	55.86±5.60	7	125.1±3.49
	Litoria pallida	2	1.50±0.21	48.89±13.18	48.65±18.19	2	110.0±32.00
	Litoria rothii	6	1.36±0.09	32.46±4.56	31.13±5.96	6	166.3±4.58
	Litoria rubella	6	0.91±0.03	29.02±1.79	17.82±1.52	6	179.8±0.17
	Litoria tornieri	8	1.70±0.07	51.01±5.23	55.41±6.95	8	160.9±7.32
	Platyplectrum ornatum	6	0.92±0.04	29.06±5.06	16.75±3.57	6	101.5±11.80
	Uperoleia lithomoda	3	0.34±0.00	13.20±2.55	3.12±0.70	3	167.7±7.22
Baoshan, Yunnan, China							
	Amolops tuberodepressus	4	1.49±0.10	36.37±6.44	36.20±7.75	5	117.0±4.74
	Babina pleuraden	6	1.39±0.11	39.22±5.41	36.86±7.74	6	78.5±6.60
	Calluella yunnanensis	1	0.71	29.00	12.37	1	82.0
	Chiromantis doriae	5	1.03±0.05	35.07±4.32	25.32±3.64	5	180.0±0.00
	Duttaphrynus melanostictus	5	0.44±0.06	7.85±2.09	2.16±0.66	5	36.6±3.33
	Hyla annectans	5	0.71±0.05	17.64±1.26	8.68±0.99	5	151.8±4.78
	Microhyla fissipes	5	1.11±0.05	42.91±8.10	32.29±9.46	5	159.0±12.60
	Nanorana yunnanensis	3	1.34±0.35	35.22±5.88	32.32±14.84	3	63.7±13.25

Odorrana grahami	6	2.05±0.10	42.63±4.59	56.89±6.43	6	68.3±2.56
Rhacophorus dugritei	5	0.77±0.12	20.13±3.52	12.12±4.40	5	156.2±6.55
Rhacophorus rhodopus	6	0.88±0.05	21.36±1.41	12.82±1.34	6	175.8±3.60
Leticia, Amazonas, Colombia						
Adenomera hylaedactyla	5	0.84±0.08	22.85±2.63	14.20±4.16	5	144.0±7.06
Allobates femoralis	1	0.91	22.74	12.31	1	172.0
Ameerega trivittata	2	1.02±0.16	21.26±3.39	15.24±3.70	2	83.0±1.00
Chiasmocleis bassleri	5	0.70±0.04	26.78±5.28	12.22±3.09	5	180.0±0.00
Dendropsophus rhodopeplus	1	1.22	41.73	28.32	1	180.0
Dendropsophus sarayacuensis	7	1.25±0.05	39.32±2.39	33.12±3.06	7	180.0±0.00
Dendropsophus triangulum	7	1.12±0.05	25.92±2.65	18.76±1.99	7	180.0±0.00
Hamptophryne boliviana	4	0.82±0.09	23.23±3.20	12.48±2.38	4	170.8±9.25
Hypsiboas hobbsi	7	1.64±0.11	36.31±3.58	43.33±6.89	7	176.6±2.57
Hypsiboas lanciformis	8	1.48±0.11	28.05±3.75	29.77±6.48	8	125.4±2.74
Hypsiboas punctatus	7	1.12±0.05	25.99±2.53	19.80±2.70	7	180.0±0.00
Leptodactylus leptodactyloides	7	1.25±0.09	36.07±4.38	30.40±5.43	7	102.4±10.01
Leptodactylus rhodomystax	8	1.39±0.04	28.18±1.60	25.58±2.08	8	48.5±2.23
Oreobates quixensis	4	1.17±0.09	38.47±8.87	31.96±6.07	4	76.5±9.91
Osteocephalus planiceps	6	1.59±0.15	28.69±3.63	32.59±7.01	6	131.3±2.92
Rhinella margaritifera	7	0.53±0.03	8.44±1.21	3.11±0.60	7	59.6±3.52
Rhinella proboscidea	2	0.46±0.11	9.12±1.76	2.84±1.13	2	87.0±22.00
Scinax ruber	6	1.12±0.09	30.66±3.96	23.47±5.15	6	169.8±6.46
Sphaenorhynchus lacteus	1	1.20	29.62	24.73	1	138.0

Table S3. Morphological data (species mean ± 1 standard error). First 10 variables (from SUL to hand) are in mm. Leg muscle mass is in grams. Metatarsal tubercle, foot webbing, toe tip, and finger tip are in mm^2. See supplementary text for variable descriptions.

Location	Species	*n*	SUL	Femur	Tibiofibula	Metatarsal	Foot
Fogg Dam, NT, Australia							
	Limnodynastes convexiusculus	5	44.01±2.07	18.99±0.73	18.38±0.88	10.00±0.46	19.96±0.65
	Litoria australis	6	68.46±1.58	34.38±0.69	32.41±0.70	16.28±0.50	28.24±0.76
	Litoria bicolor	7	25.74±0.66	12.13±0.37	12.68±0.41	6.54±0.23	9.39±0.23
	Litoria caerulea	6	73.44±1.60	32.57±0.39	31.16±0.21	17.28±0.44	28.42±0.43
	Litoria dahlii	8	53.97±1.61	26.87±0.96	26.58±1.00	13.20±0.55	26.19±1.02
	Litoria inermis	1	33.03	16.66	17.98	8.94	15.64
	Litoria longipes	6	41.67±1.40	18.29±0.62	16.45±0.54	8.72±0.36	16.99±0.66
	Litoria nasuta	7	37.55±0.58	20.82±0.34	24.33±0.58	11.56±0.28	21.32±0.52
	Litoria pallida	2	35.36±0.90	18.19±0.92	20.88±0.88	9.57±0.82	16.85±0.64
	Litoria rothii	6	45.19±0.70	23.30±0.48	23.94±0.31	11.81±0.21	19.12±0.51
	Litoria rubella	6	30.44±0.36	12.48±0.07	11.84±0.07	6.38±0.13	10.82±0.17
	Litoria tornieri	8	30.74±0.26	16.83±0.18	18.49±0.23	8.48±0.14	15.77±0.14
	Platyplectrum ornatum	6	30.89±1.59	15.30±0.97	14.22±0.73	5.84±0.45	14.85±0.85
	Uperoleia lithomoda	1	23.88±0.23	8.92±0.16	7.81±0.11	4.72±0.21	8.74±0.23
Baoshan, Yunnan, China							
	Amolops tuberodepressus	5	49.95±3.84	27.87±1.59	29.14±1.44	13.92±0.76	26.62±1.92
	Babina pleuraden	6	45.22±1.54	21.86±0.42	21.82±0.43	10.87±0.20	24.42±0.51
	Calluella yunnanensis	1	33.19	16.19	16.02	7.52	17.67
	Chiromantis doriae	5	26.49±0.77	12.14±0.48	12.66±0.48	7.37±0.39	11.54±0.54
	Duttaphrynus melanostictus	5	81.16±13.47	32.69±4.50	30.75±4.69	18.70±2.80	31.28±5.10
	Hyla annectans	5	30.20±1.01	14.53±0.47	14.60±0.47	7.95±0.22	13.74±0.53
	Microhyla fissipes	5	23.62±0.41	10.65±0.21	12.05±0.34	5.60±0.33	12.42±0.38
	Nanorana yunnanensis	3	73.53±12.05	38.89±5.02	37.29±5.44	20.18±3.17	35.21±4.72
	Odorrana grahami	6	64.57±1.08	37.94±1.21	39.76±0.70	18.74±0.44	37.43±0.71

Rhacophorus dugritei	5	39.67±1.39	18.25±0.43	16.47±0.30	8.60±0.28	17.71±0.38
Rhacophorus rhodopus	6	35.20±0.30	16.95±0.24	16.48±0.11	8.06±0.26	15.02±0.25
Leticia, Amazonas, Colombia						
Adenomera hylaedactyla	5	24.48±0.66	10.41±0.46	11.70±0.30	6.67±0.35	13.18±0.54
Allobates femoralis	1	26.96	10.96	12.66	6.20	11.82
Ameerega trivittata	2	38.97±2.90	17.83±1.61	20.25±0.89	10.76±0.55	18.21±1.18
Chiasmocleis bassleri	5	20.43±1.72	8.83±0.75	9.52±0.55	5.64±0.49	8.79±0.41
Dendropsophus rhodopeplus	1	21.82	10.76	11.94	6.61	9.03
Dendropsophus sarayacuensis	7	25.83±0.47	13.04±0.31	14.17±0.39	8.10±0.17	11.63±0.28
Dendropsophus triangulum	7	22.77±0.57	11.27±0.21	11.99±0.38	6.68±0.17	10.17±0.36
Hamptophryne boliviana	4	22.25±0.78	10.21±0.56	10.51±0.38	6.26±0.28	11.52±0.41
Hypsiboas hobbsi	7	40.56±0.70	20.50±0.21	21.27±0.33	11.98±0.28	15.60±0.33
Hypsiboas lanciformis	8	66.09±0.80	35.77±0.83	39.50±0.93	22.70±0.51	29.35±0.72
Hypsiboas punctatus	7	35.03±0.66	17.75±0.49	17.56±0.24	10.09±0.09	14.56±0.29
Leptodactylus leptodactyloides	7	32.73±1.26	15.03±0.78	16.03±0.97	8.38±0.45	18.19±0.81
Leptodactylus rhodomystax	8	75.24±3.00	35.35±1.25	36.39±1.38	17.52±0.56	37.53±1.32
Oreobates quixensis	4	39.31±3.92	20.15±2.02	21.21±1.99	10.18±1.02	20.11±1.83
Osteocephalus planiceps	6	68.11±4.79	35.00±2.49	38.45±2.68	18.05±1.41	28.19±2.16
Rhinella margaritifera	7	51.96±0.56	23.48±0.37	22.94±0.40	12.22±0.15	18.69±0.15
Rhinella proboscidea	2	41.06±9.58	18.50±4.92	17.62±4.50	9.38±2.51	14.80±3.69
Scinax ruber	6	30.79±0.60	13.74±0.27	15.04±0.32	8.64±0.27	12.70±0.24
Sphaenorhynchus lacteus	3	38.86	19.20	19.02	9.49	16.46

Location	Species	*n*	Head Length	Head Width	Humerus	Radioulna	Hand
Fogg Dam, NT, Australia							
	Limnodynastes convexiusculus	5	15.26±0.43	16.51±0.55	7.76±0.30	8.69±0.33	10.16±0.30
	Litoria australis	6	26.61±0.49	30.48±0.52	11.88±0.29	14.64±0.37	16.96±0.49
	Litoria bicolor	7	7.72±0.23	7.20±0.21	4.30±0.17	3.63±0.18	6.18±0.19
	Litoria caerulea	6	20.76±0.59	25.22±0.83	13.17±0.17	13.34±0.45	21.12±0.41

Litoria dahlii	8	16.69±0.46	16.94±0.42	9.14±0.25	9.88±0.41	13.40±0.46
Litoria inermis	1	11.48	11.41	5.41	6.35	8.27
Litoria longipes	6	14.06±0.39	16.92±0.32	6.30±0.24	9.80±0.42	10.00±0.42
Litoria nasuta	7	13.57±0.20	12.14±0.17	6.86±0.21	7.60±0.21	9.68±0.27
Litoria pallida	2	12.28±0.31	11.67±0.44	7.00±0.05	7.41±0.29	9.41±0.68
Litoria rothii	6	13.72±0.30	14.44±0.22	8.74±0.47	8.21±0.17	12.24±0.47
Litoria rubella	6	7.21±0.16	8.14±0.10	5.14±0.27	4.87±0.12	7.13±0.05
Litoria tornieri	8	10.98±0.14	10.73±0.09	5.69±0.11	6.42±0.17	7.84±0.11
Platyplectrum ornatum	6	9.46±0.43	12.23±0.60	6.30±0.55	6.71±0.59	7.64±0.54
Uperoleia lithomoda	1	5.86±0.11	7.63±0.15	4.53±0.06	4.85±0.19	5.70±0.10
Baoshan, Yunnan, China						
Amolops tuberodepressus	5	13.77±0.80	15.51±0.88	10.13±0.60	10.71±0.57	16.62±1.12
Babina pleuraden	6	14.57±0.70	15.40±0.57	6.85±0.24	7.62±0.21	11.09±0.22
Calluella yunnanensis	1	7.43	10.59	5.87	6.54	11.02
Chiromantis doriae	5	7.39±0.29	7.93±0.37	4.88±0.49	5.00±0.20	7.50±0.45
Duttaphrynus melanostictus	5	21.67±2.94	29.30±4.99	13.63±1.83	18.97±2.82	19.49±2.90
Hyla annectans	5	8.47±0.08	9.81±0.37	5.83±0.20	6.35±0.38	9.59±0.37
Microhyla fissipes	5	6.11±0.25	7.64±0.20	4.13±0.13	4.22±0.21	6.49±0.72
Nanorana yunnanensis	3	23.15±3.57	29.05±4.74	11.79±1.43	13.42±1.82	19.51±2.83
Odorrana grahami	6	20.03±0.88	22.05±0.54	13.80±0.55	14.87±0.31	19.37±0.27
Rhacophorus dugritei	5	12.03±0.52	14.74±0.34	6.89±0.28	8.87±0.35	12.53±0.34
Rhacophorus rhodopus	6	10.02±0.19	12.16±0.19	6.79±0.23	6.80±0.24	10.26±0.31
Leticia, Amazonas, Colombia						
Adenomera hylaedactyla	5	7.78±0.32	8.49±0.22	5.20±0.26	4.54±0.10	5.73±0.19
Allobates femoralis	1	8.78	8.66	6.16	6.20	6.82
Ameerega trivittata	2	10.53±0.53	10.90±0.62	10.16±0.55	9.86±0.16	11.02±0.63
Chiasmocleis bassleri	5	4.45±0.31	5.52±0.30	3.98±0.47	3.79±0.46	4.00±0.42
Dendropsophus rhodopeplus	1	6.37	7.25	5.13	4.01	5.56
Dendropsophus sarayacuensis	7	7.04±0.14	9.01±0.11	5.30±0.16	5.11±0.07	7.38±0.20

Dendropsophus triangulum	7	6.65±0.14	7.82±0.23	4.38±0.13	5.14±0.18	6.86±0.22
Hamptophryne boliviana	4	5.80±0.15	7.42±0.17	4.46±0.28	4.13±0.26	6.30±0.33
Hypsiboas hobbsi	7	11.62±0.15	14.15±0.15	8.01±0.28	8.26±0.25	12.02±0.13
Hypsiboas lanciformis	8	21.85±0.29	20.24±0.26	12.16±0.35	12.31±0.22	19.04±0.37
Hypsiboas punctatus	7	10.14±0.25	12.21±0.22	7.38±0.21	6.92±0.18	10.43±0.11
Leptodactylus leptodactyloides	7	10.11±0.39	11.46±0.48	7.24±0.26	6.19±0.25	8.78±0.43
Leptodactylus rhodomystax	8	25.55±1.13	29.99±1.43	16.64±0.81	17.68±0.75	18.60±0.62
Oreobates quixensis	4	13.24±1.59	16.07±1.74	9.29±0.89	9.49±0.86	11.04±1.10
Osteocephalus planiceps	6	21.07±1.64	21.53±1.50	12.26±0.87	14.44±1.10	20.33±1.78
Rhinella margaritifera	7	15.36±0.24	18.36±0.26	11.10±0.41	14.09±0.14	13.58±0.22
Rhinella proboscidea	2	12.34±2.41	14.39±2.85	9.64±1.14	11.11±2.44	10.65±2.09
Scinax ruber	6	9.50±0.24	10.01±0.22	5.47±0.20	5.69±0.19	7.77±0.15
Sphaenorhynchus lacteus	3	7.93	11.64	7.76	7.33	11.04

Location	Species	*n*	Leg muscle mass	Metatarsal tubercle	Foot webbing	Toe tip	Finger tip
Fogg Dam, NT, Australia							
	Limnodynastes convexiusculus	5	0.402±0.063	2.51±0.46	0.85±0.19	3.24±0.18	2.28±0.06
	Litoria australis	6	2.040±0.236	6.81±0.38	22.14±3.18	8.64±0.64	6.01±0.56
	Litoria bicolor	7	0.039±0.004	0.31±0.03	6.70±0.38	3.36±0.21	3.02±0.18
	Litoria caerulea	6	1.123±0.114	4.80±0.39	64.73±3.90	49.21±4.39	52.93±4.58
	Litoria dahlii	8	0.842±0.109	2.57±0.23	130.96±11.46	6.26±0.57	3.53±0.15
	Litoria inermis	1	0.202	0.99	14.16	1.76	0.83
	Litoria longipes	6	0.241±0.033	2.37±0.12	4.16±0.54	3.71±0.32	3.26±0.21
	Litoria nasuta	7	0.332±0.028	1.36±0.18	24.88±1.74	4.67±0.34	3.09±0.22
	Litoria pallida	2	0.297±0.032	1.14±0.32	22.55±2.07	2.67±0.14	2.27±0.62
	Litoria rothii	6	0.302±0.024	1.35±0.08	52.45±7.98	14.05±0.74	14.65±1.06
	Litoria rubella	6	0.062±0.004	0.55±0.05	4.81±0.30	4.63±0.28	4.72±0.12
	Litoria tornieri	8	0.157±0.012	0.98±0.10	10.93±0.90	2.12±0.15	1.67±0.17
	Platyplectrum ornatum	6	0.192±0.037	2.18±0.42	8.89±1.95	2.66±0.60	1.93±0.14

Uperoleia lithomoda	1	0.044±0.003	2.08±0.04	0.79±0.09	0.86±0.10	0.52±0.04
Baoshan, Yunnan, China						
Amolops tuberodepressus	5	0.724±0.187	2.78±0.39	72.75±9.70	17.18±2.79	18.02±1.47
Babina pleuraden	6	0.590±0.086	2.01±0.21	16.29±2.07	4.27±0.53	2.59±0.34
Calluella yunnanensis	1	0.250	3.54	22.29	2.11	1.86
Chiromantis doriae	5	0.036±0.010	0.31±0.08	1.61±0.25	3.54±0.54	4.25±0.72
Duttaphrynus melanostictus	5	3.906±1.820	10.29±3.24	24.91±6.21	12.43±4.19	13.01±4.27
Hyla annectans	5	0.028±0.006	0.75±0.02	5.53±0.73	4.05±0.42	4.40±0.39
Microhyla fissipes	5	0.054±0.006	0.58±0.03	0.77±0.16	1.64±0.25	1.45±0.12
Nanorana yunnanensis	3	4.433±1.918	8.17±1.07	157.84±49.99	12.63±3.99	9.78±1.67
Odorrana grahami	6	2.205±0.171	4.18±0.52	198.20±14.48	15.82±0.58	9.92±0.50
Rhacophorus dugritei	5	0.118±0.017	1.64±0.12	9.64±1.86	10.14±1.67	12.39±0.88
Rhacophorus rhodopus	6	0.047±0.005	0.98±0.07	24.02±2.26	7.80±0.48	9.95±0.84
Leticia, Amazonas, Colombia						
Adenomera hylaedactyla	5	0.092±0.012	0.48±0.05	0.15±0.04	1.61±0.15	0.84±0.13
Allobates femoralis	1	0.122	0.76	0.66	3.89	2.15
Ameerega trivittata	2	0.345±0.082	1.63±0.15	0.37±0.03	5.81±0.14	4.35±0.34
Chiasmocleis bassleri	5	0.047±0.008	0.22±0.08	0.09±0.02	1.71±0.25	0.53±0.15
Dendropsophus rhodopeplus	1	0.035	0.31	8.54	2.96	3.66
Dendropsophus sarayacuensis	7	0.058±0.003	0.56±0.08	12.39±0.61	5.23±0.52	4.88±0.32
Dendropsophus triangulum	7	0.039±0.003	0.42±0.06	11.38±0.84	4.69±0.54	4.16±0.26
Hamptophryne boliviana	4	0.075±0.010	0.67±0.13	0.33±0.04	2.19±0.12	1.36±0.09
Hypsiboas hobbsi	7	0.649±0.397	1.94±0.09	36.29±2.12	11.17±0.48	10.77±0.56
Hypsiboas lanciformis	8	1.228±0.040	2.59±0.15	85.36±3.09	24.10±0.50	23.30±0.56
Hypsiboas punctatus	7	0.096±0.007	0.90±0.09	11.15±0.77	8.56±0.55	8.81±0.34
Leptodactylus leptodactyloides	7	0.302±0.051	1.12±0.07	1.03±0.20	2.55±0.38	1.78±0.30
Leptodactylus rhodomystax	8	3.037±0.304	6.23±0.56	3.85±0.97	14.16±1.82	11.43±1.58
Oreobates quixensis	4	0.447±0.105	1.84±0.44	0.21±0.08	2.63±0.57	2.15±0.37
Osteocephalus planiceps	6	1.332±0.278	4.34±0.67	81.77±13.76	33.08±5.80	37.80±6.44

Rhinella margaritifera	7	0.510±0.030	3.40±0.32	11.41±1.20	6.03±0.58	4.95±0.43
Rhinella proboscidea	2	0.267±0.195	1.93±0.46	8.01±4.50	5.44±1.83	3.84±2.12
Scinax ruber	6	0.093±0.007	0.55±0.05	12.79±1.48	6.87±0.40	6.72±0.36
Sphaenorhynchus lacteus	3	0.296	1.38	36.19	14.55	12.82

Table S4. Results of phylogenetic principal components analysis. The phylogeny used for this analysis was the time-calibrated tree from BEAST in which the topology was constrained to match the topology of Pyron and Wiens [S42].

(a) Morphology

	PC1	PC2	PC3	PC4	PC5	PC6	PC7	PC8	PC9	PC10
Eigenvalues	8.277	0.882	0.473	0.146	0.094	0.047	0.032	0.020	0.016	0.012
Percent of total variation	82.77	8.82	4.73	1.46	0.94	0.47	0.32	0.20	0.16	0.12

Eigenvectors

Original variable	PC1	PC2	PC3	PC4	PC5	PC6	PC7	PC8	PC9	PC10
Snout-to-urostyle length	0.342	0.103	-0.065	-0.089	0.019	-0.059	-0.386	-0.810	-0.167	0.152
Leg length	0.339	0.095	0.042	-0.398	-0.096	-0.455	0.023	0.173	-0.337	-0.597
Head length	0.328	0.247	-0.085	-0.400	0.445	0.193	0.263	0.235	-0.255	0.489
Head width	0.332	0.242	-0.104	0.123	0.404	0.405	-0.059	-0.017	0.466	-0.507
Arm length	0.342	0.038	-0.094	0.096	-0.002	-0.626	-0.057	0.159	0.584	0.321
Leg mass	0.326	0.246	0.079	-0.113	-0.756	0.332	0.308	-0.036	0.175	0.077
Tubercle area	0.321	0.245	0.072	0.768	-0.033	-0.029	-0.061	0.206	-0.438	0.047
Foot webbing area	0.250	-0.357	0.881	-0.015	0.144	0.060	0.023	-0.029	0.075	0.039
Toe tip area	0.296	-0.503	-0.252	-0.114	-0.176	0.285	-0.573	0.367	-0.052	0.071
Finger tip area	0.272	-0.598	-0.340	0.185	0.073	-0.029	0.589	-0.232	-0.069	-0.083

(b) Performance

	PC1	PC2	PC3	PC4	PC5	PC6	PC7	PC8
Eigenvalues	4.509	1.282	1.111	0.579	0.322	0.151	0.036	0.010
Percent of total variation	56.37	16.02	13.89	7.24	4.02	1.89	0.45	0.12

Eigenvectors

Original variable	PC1	PC2	PC3	PC4	PC5	PC6	PC7	PC8
Jump - peak velocity	0.410	0.133	0.291	-0.192	0.308	-0.686	0.118	0.335
Jump - peak acceleration	0.386	0.336	-0.191	-0.259	-0.520	0.226	0.535	0.164
Jump - peak power	0.417	0.318	0.088	-0.297	-0.155	0.046	-0.655	-0.417
Jump - takeoff angle	0.271	0.423	0.147	0.846	0.049	0.088	0.017	-0.014
Swim - peak velocity	0.419	-0.281	0.004	-0.068	0.511	0.263	0.385	-0.511
Swim - peak acceleration	0.291	-0.498	-0.380	0.291	-0.418	-0.464	-0.037	-0.214
Swim - peak power	0.414	-0.357	-0.142	0.038	0.131	0.408	-0.340	0.616
Maximum clinging angle	-0.055	0.367	-0.827	-0.030	0.393	-0.129	-0.071	0.023

Table S5. Two-block partial least squares (2B-PLS) analysis of the overall relationship between morphology and performance. All "relative" morphological variables were residual values from a phylogenetic regression of the raw values on snout-to-urostyle length. Coefficients in bold are those that represent the primary relationship between morphology and performance along each 2B-PLS dimension. Singular values represent the total covariance between morphology and performance in each dimension and correlation corresponds to this singular value – the correlation between morphology and performance in that dimension.

		Dimensions		
Matrix	Variable	1	2	3
$\mathbf{F}_1$	Snout-to-urostyle length	-0.149	**-0.450**	**0.838**
	Relative leg length	**0.701**	-0.166	-0.024
	Relative head length	0.319	-0.315	-0.001
	Relative head width	-0.120	-0.207	0.038
	Relative arm length	-0.145	0.139	0.164
	Relative leg mass	0.242	-0.374	-0.245
	Relative tubercle area	-0.348	-0.125	-0.271
	Relative foot webbing area	0.329	0.087	0.173
	Relative toe tip area	0.200	**0.469**	0.208
	Relative finger tip area	0.146	**0.475**	0.251
$\mathbf{F}_2$	Jump - peak velocity	**0.408**	-0.073	**0.369**
	Jump - peak acceleration	**0.350**	-0.061	**-0.597**
	Jump - peak power	**0.409**	-0.030	-0.166
	Jump - takeoff angle	0.045	-0.400	**-0.437**
	Swim - peak velocity	**0.415**	-0.068	**0.451**
	Swim - peak acceleration	**0.388**	-0.127	-0.168
	Swim - peak power	**0.415**	-0.088	0.154
	Maximum clinging angle	0.218	**0.895**	-0.186
Singular value		2.564	1.238	0.839
Correlation		0.585	0.662	0.556

Table S6. Effect sizes of phylogenetic MANOVA relating morphology and performance to microhabitat use (two models run separately).

Morphology

	PC2	PC3	PC4	PC5	PC6	PC7	PC8	PC9	PC10
arboreal	-0.887	0.031	-0.096	0.071	0.008	-0.005	-0.024	0.019	-0.020
burrowing	0.683	0.333	0.568	0.145	0.041	0.023	0.043	-0.040	0.021
semi-aquatic	0.684	0.798	-0.247	-0.127	0.096	0.028	-0.090	-0.052	-0.006
terrestrial	0.436	-0.280	-0.081	-0.045	-0.035	0.005	0.030	0.019	0.023

Performance

	PC2	PC3	PC4	PC5	PC6	PC7	PC8
arboreal	0.083	-0.425	-0.175	0.384	-0.152	-0.014	-0.010
burrowing	0.301	0.778	-0.005	-0.339	0.090	0.059	-0.021
semi-aquatic	-1.060	0.303	0.718	-0.319	0.201	0.068	0.022
terrestrial	0.037	0.137	-0.017	-0.180	0.060	-0.030	0.004

Table S7. Comparison of *Litoria* in novel microhabitats to other species of frogs using similar microhabitats and to other *Litoria* in the ancestral microhabitat (arboreal). (a) Test of history: distance between arboreal *Litoria* and *Litoria* in the novel microhabitat (D_{obs}), arboreal *Litoria* and unrelated species in the novel microhabitat (D_{exp}), and P_{sim} estimated via simulation. "Global P_{sim}" represents whether *Litoria* in novel microhabitats as a whole are closer in PC space to arboreal *Litoria* than the latter is to unrelated species in the novel microhabitat. (b) First convergence test: distance between *Litoria* in the novel microhabitat and other species in that microhabitat (D_{env}), the former with *Litoria* in the ancestral, arboreal microhabitat (D_{obs}), and P_{sim} estimated via simulation. (c) Second convergence test: r_{vec} is the vector correlation between the observed and expected divergence vectors (the proportion of total divergence from arboreal *Litoria* that is along the expected trajectory of divergence), angles (θ, in degrees) are those between these two vectors, and P_{sim} was calculated via simulation. Global P_{sim} in (b) and (c) are as in (a).

(a) Test of history

	Morphology			Performance		
	D_{exp}	D_{obs}	P_{sim}	D_{exp}	D_{obs}	P_{sim}
burrowing	20.17	18.54	0.820	11.85	18.78	0.974
semi-aquatic	16.34	16.33	0.799	17.57	25.37	0.940
terrestrial	16.02	16.02	0.708	11.74	11.21	0.703
	Global P_{sim} = 0.5231			Global P_{sim} = 0.6638		

(b) Test of convergence: distances

	Morphology			Performance		
	D_{env}	D_{obs}	P_{sim}	D_{env}	D_{obs}	P_{sim}
burrowing	11.64	18.54	0.017	12.82	18.78	0.021
semi-aquatic	9.41	16.33	0.016	12.17	25.37	0.007
terrestrial	13.74	16.02	0.113	11.13	11.21	0.157
	Global P_{sim} = 0.0002			Global P_{sim} = 0.0001		

(c) Test of convergence: vector correlation

	Morphology			Performance		
	r_{vec}	θ	P_{sim}	r_{vec}	θ	P_{sim}
burrowing	0.822	34.68	0.065	0.738	42.40	0.102
semi-aquatic	0.834	33.48	0.055	0.902	25.53	0.020
terrestrial	0.632	50.78	0.202	0.530	57.96	0.247
	Global P_{sim} = 0.0003			Global P_{sim} = 0.0025		

Figure S1. Principal components scores for morphology, plotted for PC2–4, which show the greatest amount of non-size-related variation among species. Colors indicate microhabitat use of each species, while symbol shape indicates from which assemblage it comes. PC2 represented shared variation in the size of toe and fingertips as well as foot webbing, with larger values in PC space corresponding to smaller absolute values. PC3 largely represented variation in foot webbing, partly as a contrast with toe and fingertips. Finally, PC4 primarily showed large negative weights for head and leg length, contrasted with a large positive weight for metatarsal tubercle size.

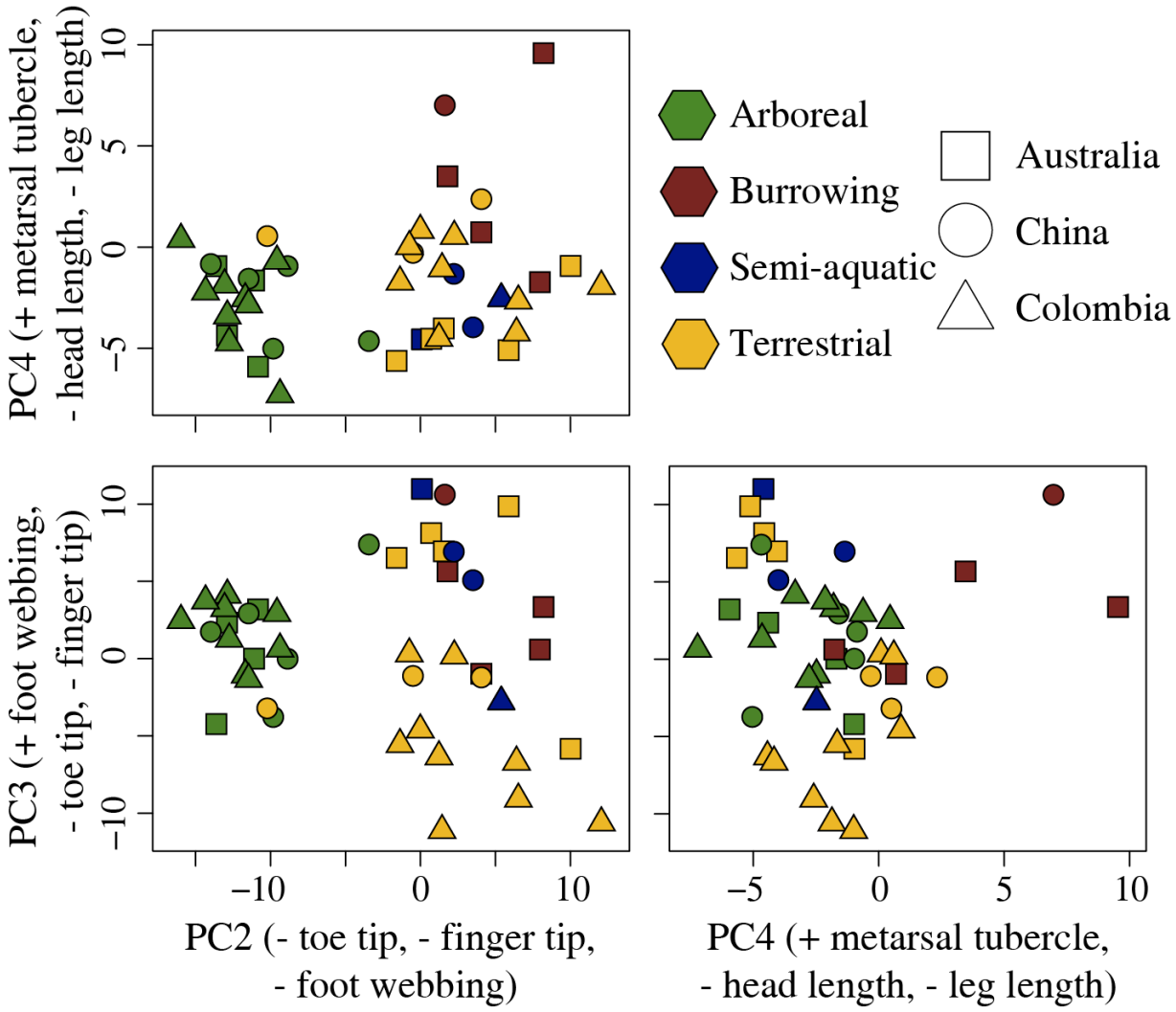

Figure S2. Principal components scores for performance, plotted for PC2–4, which show the greatest amount of variation among species beyond a general high-performance axis (PC1). Colors indicate microhabitat use of each species, while symbol shape indicates from which assemblage it comes. PC2 showed a contrast between jumping and clinging performance versus swimming performance (i.e. peak jumping acceleration, peak jumping power, jumping angle, and clinging angle, versus peak swimming velocity, peak swimming acceleration, and peak swimming power). PC3 largely represented variation in clinging angle, while PC4 represented variation in jumping takeoff angle.

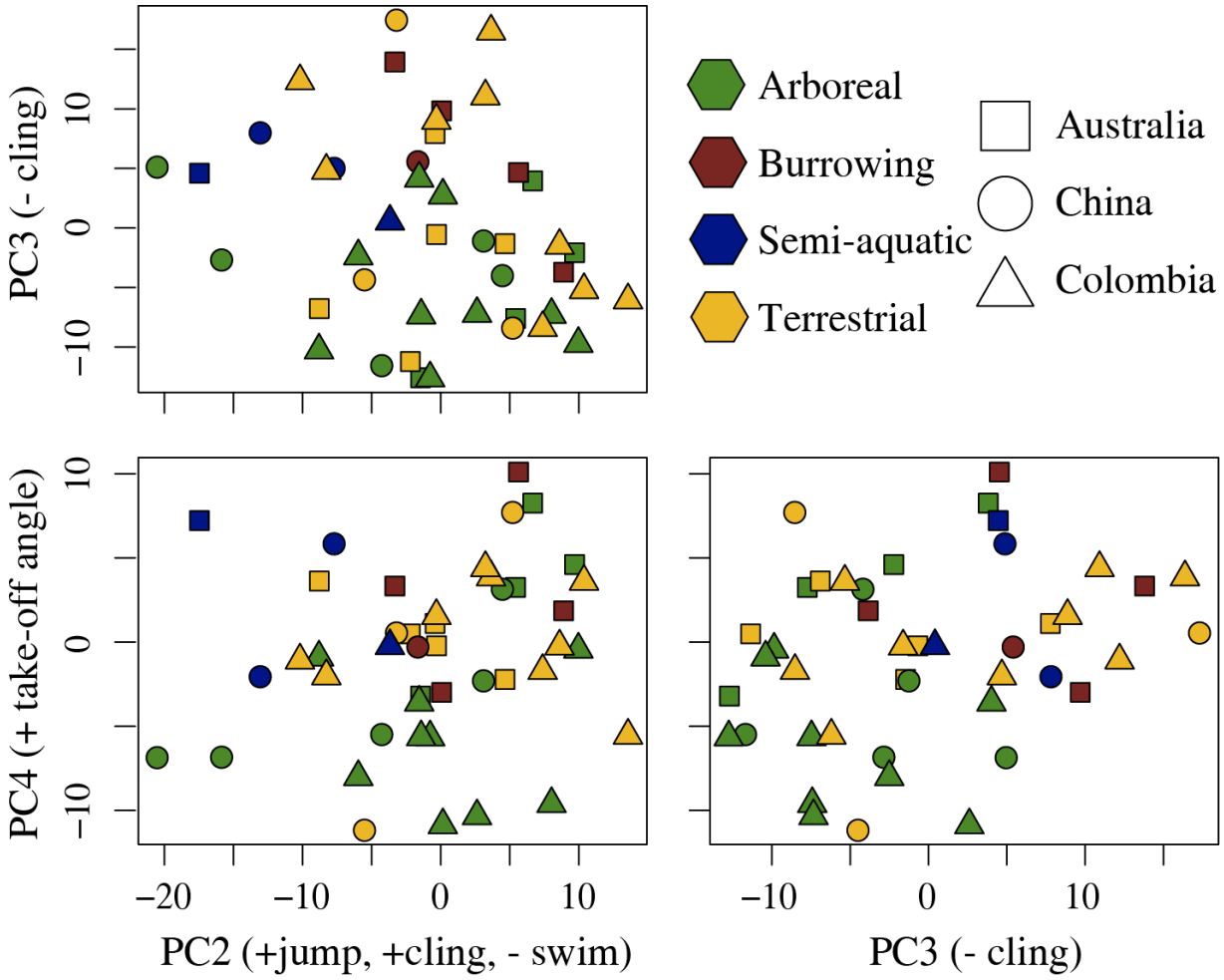

Figure S3. Ancestral-state estimation of microhabitat use in frogs, estimated by unordered, equal-rates maximum-likelihood [S90] in R with the package *diversitree* [S91]. Proportional size of the microhabitat color of the pie at each node is directly proportional to likelihood of that state at that node [S90]. At the bottom it can be seen that the ancestral microhabitat use of *Litoria* was mostly likely arboreal (proportional likelihood = 0.938). This is supported by the fact that its sister group Phyllomedusinae, which we did not study here, is a clade of 61 species that are all arboreal [S81].